UNIVERSITÀ DEGLI STUDI
DI TRENTO

CIMeC - Center for Mind/Brain Sciences

Phd Dissertation

Novel data-driven analysis methods for real-time fMRI and simultaneous EEG-fMRI neuroimaging

Author:
Nicola Soldati

Supervisors:
Dr. Jorge Jovicich
Prof. Lorenzo Bruzzone

A thesis submitted for the degree of
PhilosophiæDoctor (PhD)
Doctoral School in Cognitive and Brain Sciences

XXIV cycle

December, 2012

To my family

Acknowledgements

A journey coming to an end always leaves behind itself a long path of moments and people filling them. This PhD path permitted to me to live plenty of good (and less good) moments, in which I encountered several people who have been very important to me. Starting from the beginning I need to be very grateful to my PhD advisors Jorge Jovicich and Lorenzo Bruzzone, whose mentoring always followed me in all the steps toward this goal. I also need to thank Christina Tryantafillou and Oliver Hinds, for having introduced me to the practice of real-time fMRI in my firsts uncertain steps. Great efforts into improving my expertises on ICA knowledge have been sustained by Vince Calhoun, whose help has been a key feature of this work. Finally a special mention goes to Andrzej Cichocki for the warm hospitality that he made me feel, the precious help and good time in a far away country and the high level profile of the research done at his laboratory. A special thank is for Sara Assecondi, who always generously offered her expertise and data to support my research.

In all the above mentioned laboratories I also found always very good friends, who made the journey less difficult and helped me a lot with practical issues and theoretical discussions. Although mentioning everyone would be impossible I would like to particularly thanks Elena Allen, Siddharth Khullar and Martin Havlicek from MIAlab and Qibin Zhao, Huy Phan Anh and Guoxu Zhou, from the Cichocki Laboratory. All of them helped me, I hope with exchange, in working better on my projects.

I would like to acknowledge all my old friends, who made me feel where home was when I was far away. And a special person who taught me that home is not always in a fixed place.

I thank my companions of PhD course Vittorio, Francesca, Anne, Marianna, Laura, Elisa and Francesca (no, is not a typo, is another Francesca). My flatmate Andrea, I think he will be tired to hear my thanksgiving, and my old friend Luca and Maria.

I thank specially Mauro, who made a journey parallel to mine and Gianandrea, who found a small flower along his one.

I need to thank also everyone not mentioned here, but whose presence has been determinant to my life and who made my journey worth to be accomplished.

Finally, but the most important, I thank my family (included new entries)... it is due to their efforts that I could do what I did.

We cannot direct the wind, but we can adjust the sails.

Dolly Parton

Abstract

Real-time neuroscience can be described as the use of neuroimaging techniques to extract and evaluate brain activations during their ongoing development. The possibility to track these activations opens the doors to new research modalities as well as practical applications in both clinical and everyday life. Moreover, the combination of different neuroimaging techniques, i.e. multimodality, may reduce several limitations present in each single technique. Due to the intrinsic difficulties of real-time experiments, in order to fully exploit their potentialities, advanced signal processing algorithms are needed. In particular, since brain activations are free to evolve in an unpredictable way, data-driven algorithms have the potentials of being more suitable than model-driven ones. In fact, for example, in neurofeedback experiments brain activation tends to change its properties due to training or task effects thus evidencing the need for adaptive algorithms. Blind Source Separation (BSS) methods, and in particular Independent Component Analysis (ICA) algorithms, are naturally suitable to such kind of conditions. Nonetheless, their applicability in this framework needs further investigations.

The goals of the present thesis are: i) to develop a working real-time set up for performing experiments; ii) to investigate different state of the art ICA algorithms with the aim of identifying the most suitable (along with their optimal parameters), to be adopted in a real-time MRI environment; iii) to investigate novel ICA-based methods for performing real-time MRI neuroimaging; iv) to investigate novel methods to perform data fusion between EEG and fMRI data acquired simultaneously.

The core of this thesis is organized around four "experiments", each one addressing one of these specific aims. The main results can be summarized as follows.

Experiment 1: a data analysis software has been implemented along with the hardware acquisition set-up for performing real-time fMRI. The set-up has been developed with the aim of having a framework into which it would be possible to test and run the novel methods proposed to perform real-time fMRI.

Experiment 2: to select the more suitable ICA algorithm to be implemented in the system, we investigated theoretically and compared empirically the performance of 14 different ICA algorithms systematically sampling different growing window lengths, model order as well as a priori conditions (none, spatial or temporal). Performance is evaluated by computing the spatial and temporal correlation to a target component of brain activation as well as computation time. Four algorithms are identified as best performing without prior information (constrained ICA, fastICA, jade-opac and evd), with their corresponding parameter choices. Both spatial and temporal priors are found to almost double the similarity to the target at not computation costs for the constrained ICA method.

Experiment 3: the results and the suggested parameters choices from experiment 2 were implemented to monitor ongoing activity in a sliding-window approach to investigate different ways in which ICA-derived a priori information could be used to monitor a target independent component: i) back-projection of constant spatial information derived from a functional localizer, ii) dynamic use of temporal , iii) spatial, or both iv) spatial-temporal ICA constrained data. The methods were evaluated based on spatial and/or temporal correlation with the target IC component monitored, computation time and intrinsic stochastic variability of the algorithms. The results show that the back-projection method offers the highest performance both in terms of time course reconstruction and speed. This method is very fast and effective as far as the monitored IC has a strong and well defined behaviour, since it relies on an accurate description of the spatial behaviour. The dynamic methods offer comparable performances at cost of higher computational time. In particular the spatio-temporal method performs comparably in terms of computational time to back-projection, offering more

variable performances in terms of reconstruction of spatial maps and time courses.

Experiment 4: finally, Higher Order Partial Least Square based method combined with ICA is proposed and investigated to integrate EEG-fMRI data acquired simultaneously. This method showed to be promising, although more experiments need to be done in order to fully quantify its performance and stability.

Contents

List of Figures

List of Tables

Glossary

BCI Brain Computer Interface; term which indicate an interface directly coupling brain activity with periphery systems through computer

BOLD Blood Oxygenation Level Dependent; signal measured by fMRI, due to the concentration of oxygen in the blood

BSS Blind Source Separation; signal processing techniques to extract information content present in data exploiting minimal assumption and knowledge of the data themselves

DAQ Data Acquisition; fieldtrip buffer

EEG Electroencephalography; Neuroimaging technique based on acquisition of brain electrical signal

FL Functional Localizer; typical step of a real-time system consisting of the identification of the brain function of interest

fMRI functional Magnetic Resonance Imaging; Neuroimaging technique based on acquisition of brain haemodynamic mediated signal

HOPLS Higher Order Partial Least Square; tensorial extension of PLS

ICA Independent Component Analysis; BSS technique based on statistical properties of independence of the sources present in the data

PLS Partial Least Square; advanced technique to associate datasets through the use of latent variable as predictors

TBV Turbo Brain Voyager; commercial software to run real-time fMRI experiments

1

Introduction

1.1 Outline

Real-time neuroscience is a promising technology for the development of new research modalities as well as practical applications in both clinical and everyday life. Indeed measuring the brain signal in real-time would permit not only to monitor it better and to timely adjust the research paradigm, but also to exploit it directly for the control of an external device such as cursors or rehabilitation devices or neuroprosthesis. Historically, due to practical issues such as portability and low cost, Electroencephalography (EEG) has been the most investigated neuroimaging technique for the implementation of real-time systems. For this reason a huge amount of literature has been produced proposing many different approaches to the realization of a real-time system. In particular, in the framework of Brain Computer Interface (BCI) many advanced feature extraction, feature selection and classification techniques have been implemented from machine learning and pattern recognition fields (Bashashati et al., 2007).

Brain Computer Interface (BCI) is by far the most investigated topic in which real-time neuroscience is adopted, since its application greatly improves the quality of life and reduce social cost for impaired patient. Using BCI a patient would be able for example to have a new communication channel which permits even to locked-in syndrome patients to communicate with external world (Sorger et al., 2012). The classical structure of a real-time system foresees the collaborative functioning of three different steps: i) the signal acquisition, 2) the signal analysis, and 3) the signal exploitation. The signal acquisition deals with the neuroimaging technique adopted, the data analysis is

devoted to the processing and monitoring of the acquired signal in order to extract the behaviour of interest and, finally, the actuation means how the behaviour of interest is exploited (i.e. visualization, BCI, monitoring). In general the more the data analysis step is accurate and reliable, the better relevant information can be extracted in a robust way, resulting thus in a system less prone to errors.

Recently a great attention has been posed on how to exploit also functional Magnetic Resonance Imaging (fMRI) technique in real-time analysis, and a growing number of publications addresses possible solutions to this problem. Given that real-time fMRI is still in its early stage, only few data analysis techniques have been proposed in the literature, since the first and most targeted problem was to reach a full technical feasibility (Cox et al., 1995). Once the technical feasibility has been demonstrated the focus moved on the implementation of data analysis algorithms suitable for the constraints of real-time fMRI. The majority of initial studies used regression based methods such as General Linear Model, followed by some more advanced techniques such as Support Vector Machine (SVM) based classifier (LaConte et al., 2007) and Multi-Voxel Pattern Analysis (MVPA) methods. Blind Source Separation (BSS) algorithms, such as Independent Component Analysis (ICA) (Calhoun and Adali, 2006) are promising, yet not adequately investigated. ICA techniques extract intrinsic characteristics of the measured data without the need of a brain activity model. Such data-driven methods not only have the advantage of detecting brain networks that may have been missed by a model, but are also particularly effective in cases where no model can be defined, like in resting state studies or in cases where the brain activation of interest changes its own behaviour during the experiment (which is a typical case for real-time neuroscience).

The exploitation of fMRI as a real-time neuroimaging technique suffers of some intrinsic limitations due to the biophysical nature of its signal. In fact, although being characterized by a very high spatial resolution, the haemodynamic filtered nature of the Blood Oxygen Level Dependent (BOLD) signal is a constraint for the temporal resolution which can be obtained. This constraint results into an additional delay in time of several seconds between the time onset of the brain activity and the actual measurable activation. The delay has to be added to acquisition and reconstruction of the brain volume using magnetic resonance imaging and to that of the data analysis

algorithms adopted. This is the counterpart of having a high spatial resolution neuroimaging technique such as fMRI. For this reason a solution to improve both spatial and temporal resolution has been seen in literature as the joint exploitation of different techniques. Combining different neuroimaging techniques is a solution known as multimodal neuroimaging. Recently EEG and fMRI techniques for neuroimaging were combined, permitting to acquire simultaneously the data from both the modalities.

This thesis proposes to study real-time neuroimaging systems in terms of both realization of technical hardware and software set-up and in terms of evaluating, developing and proposing novel techniques for advanced signal processing. Novel methodologies for real-time fMRI based on Independent Component Analysis (ICA) are presented and validated, along with methods for the fusion of information from multimodal EEG-fMRI brain signal acquisitions.

The structure of the thesis is as follows.

In the first part of the dissertation, *Chapter 2* and *3* describe the theoretical foundations of neuroimaging techniques adopted in the studies (*Chapter 2*) along with the general description of real-time neuroscience principles (*Chapter 3*).

Chapter 4 contains the first and basic study performed, which is the implementation of a working real-time fMRI framework and set-up along with the technical details on hardware and software adopted in our facility. For ease of completeness, a comprehensive set-up for real-time EEG-fMRI is presented underlying both the parts fully developed and those only tested.

In *Chapter 5* the second experiment is presented. This part of the thesis analyses different ICA algorithms in order to explore their properties in ill-posed conditions such as those offered by real-time constraints (i.e. limited data, dynamic changes in the data and computational speed). In our comparison we investigate and compare the performance of 14 different ICA algorithms systematically sampling different growing window lengths, model order as well as a priori conditions (none, spatial or temporal). The best performing algorithms in real-time constraints will be exploited in the third

experiment presented in *Chapter 6*.

In *Chapter 6* we exploited the results obtained by *Chapter 5* to propose novel implementations to use ICA-based analysis methods as an effective trade-off between data interpretability and information extraction. In this chapter we evaluated the performance of several ICA-based algorithms for monitoring dynamic brain activity by simulating a real-time fMRI experiment with real fMRI data. Algorithms were implemented to monitor ongoing activity in a sliding-window approach and differed in the ways that ICA-derived a priori information was used to monitor a target independent component (IC): i) back-projection of constant spatial information derived from a functional localizer, ii) dynamic use of temporal, iii) spatial, or both iv) spatial-temporal ICA constrained data. The methods were evaluated based on spatial and/or temporal correlation with the target IC component monitored, computation time and intrinsic stochastic variability of the algorithms.

Chapter 7 presents the fourth and last experiment, where a novel approach to the data fusion of EEG and fMRI is proposed, within an information theory perspective. The proposed method is based on Higher Order Partial Least Square (HOPLS), a recent extension of Partial Least Square (PLS) technique which is based on the exploitation of tensors and Tensorial Decomposition (TD) algorithms instead of data of lower dimensionality. The aim is to find common latent variables between two different tensorial datasets, in this case EEG and fMRI data, which maximize covariance.

We test the procedure on experimental data from a jointly acquired EEG-fMRI dataset. The dataset was recorded by Sara Assecondi at our facility within a research project unrelated to the present thesis. The dataset was acquired from healthy subjects, in a scanner at 4T and with a 64 channels EEG cap.

In *chapter 8* we summarize the work, drawing conclusions on the main results and proposing future lines of research.

1.2 Main Contributions

The entire work presented in this thesis has been realized in the Laboratory for the Functional Neuroimaging (Lnif) within the Interdepartmental Center for Brain/Mind Sciences (CIMeC, University of Trento) with extensive collaborations with the Remote Sensing Laboratory group (RSLab) within the department of Telecommunication Engineering (University of Trento). Within the duration of the PhD activity, external collaborations have been set-up with worldwide recognized labs, where the author has been accepted for short periods as visiting researcher. These institutions are the John Gabrieli Lab, Massachusetts Institute of Technology, USA; the MIAlab ruled by prof. Vince Calhoun, University of New Mexico,USA and the Andrzej Cichocki Lab, Brain Science Institute Riken, Japan. The work performed during the PhD resulted in published works as well as several proceedings, in national and international conferences, both as first author or co-author, A list of author's publications is provided in the following.

1.2.1 International Journals

Published

N. Soldati, S. Robinson, C. Persello, J. Jovicich, L. Bruzzone, "Automatic Classification of Brain Resting States using fMRI Temporal Signals". IEE Electronics Letters, 2009, 45(1), p. 19-21.

S. Robinson, G. Basso, **N. Soldati**, U. Sailer, J. Jovicich, L. Bruzzone, I. Kryspin Exner, H. Bauer, and E. Moser. The resting state of the basal ganglias motor control circuit. BMC Neuroscience, 2009, 10:137 (23 November 2009).

Submitted:

N. Soldati, V. Calhoun, L. Bruzzone, J. Jovicich, Data driven real-time brain fMRI with ICA: an evaluation of performance as function of algorithms, parameters and a priori conditions, Frontiers of Human Neuroscience.

N. Soldati, V. Calhoun, L. Bruzzone, J. Jovicich, The use of a priori information in ICA-based techniques for real-time fMRI: an evaluation of static/dynamic and spatial/temporal characteristics, Frontiers of Human Neuroscience.

1.2.2 Conferences and Workshops

Abstracts with poster presentation

S. Robinson, **N. Soldati**, G. Basso, U. Sailer, J. Jovicich, L. Bruzzone, I. Kryspin Exner, H. Bauer, and E. Moser, A Resting State Network in the Basal Ganglia, International Society of Magnetic Resonance in Medicine; Toronto, Canada; 2008.

N. Soldati, S. Robinson, L. Bruzzone, J. Jovicich, Automatic Identification of Human Brain Resting State Networks: Reliability of Classification Over Number of Independent Components Identified, Organization of Human Brain Mapping, San Francisco, USA, 2009.

N. Soldati, S. Robinson, G. Basso, L. Bruzzone, J. Jovicich, Brain Resting State fMRI Independent Components: Spectral Consistency Within Group, Organization of Human Brain Mapping, Barcelona, Spain, 2010.

N. Soldati, O. Hinds, C. Tryantafillou, J. Jovicich, Timing Resting State Networks dynamics for Real-Time fMRI Analysis, Organization of Human Brain Mapping, Barcelona, Spain, 2010.

N. Soldati, O. Hinds, C. Triantafyllou, J. Jovicich, Preliminary Investigation of RSN dynamics for rtfMRI Analysis, Poster Award, Risonanza Magnetica in Medicina, dalla Ricerca Tecnologica Avanzata alla Pratica Clinica. ISMRM Italian Chapter, Milan, Italy, 2010.

N. Soldati, S. Robinson, G. Basso, L. Bruzzone, J. Jovicich, Evaluation of Consistency in Group Independent Component Analysis of Brain Resting State fMRI Exploiting Automatic Spectral Classification Criteria, ISMRM Italian Chapter, Milan, Italy,

2010.

N. Soldati, V. Calhoun, L. Bruzzone, J. Jovicich, Real-time fMRI using ICA: optimization study for defining a target IC from a functional localizer, Organization of Human Brain Mapping, Beijing, China, 2012.

N. Soldati, V. Calhoun, L. Bruzzone, J. Jovicich, Real-time fMRI using ICA: optimization study for dynamically monitoring a target IC with different types of a priori information, Organization of Human Brain Mapping, Beijing, China, 2012.

1.2.3 Talks

International

N. Soldati, Real-Time fMRI: Signal Processing Perspectives, Invited Talk, Tokyo Institute of Technology, Tokyo, Japan, 2012.

N. Soldati, Group Independent Component Analysis of Brain Resting State fMRI, Invited Talk, FENSIBRO, Lausanne, Switzerland, 2011.

N. Soldati, Perspectives on Multi-Variate Data Analysis, Invited Talk, MIAlab, The Mind Research Institute, Albuquerque, USA, 2011.

N. Soldati, Evaluation of Consistency in Group Independent Component Analysis of Brain Resting State fMRI Exploiting Automatic Spectral Classification Criteria, Invited Talk, ISMRM Italian Chapter, Milan, Italy, 2010.

2

Physiology of the signal

2.1 Electroencephalography

In this section a brief description of the generative model for the EEG signal is described, along with the main properties of the signal acquisition system from a physical point of view.

2.1.1 Source of the signal

The generative model behind the EEG signal is strictly related to the electrical characteristics of the physiology of the brain both at a microscopic and at a macroscopic level. The current state of the art knowledge of the generation of the electrical signal affirms that the neurons are characterized by their electrical behaviour (Menon and Crottaz-Herbette, 2005; Mulert and Lemieux, 2009; Ullsperger and Debener, 2010). More in detail they respond to different stimuli by triggering two different types of induced currents. At the microscopic level the basic electrical signal is triggered by the neurons, in which the Sodium-Potassium pump induces a ionic dendritic current at a cellular level. This current rapidly spikes and propagates along the axon of the neuron, induced by rapid action potentials. These action potentials, i.e. Multi Unit Activity (MUA), are characterized by the fact of being strong (80mV), fast (<2ms), with high dynamic (300 Hz) and well localized, since their potential decays of a magnitude order within a radius of 50 μm. Due to this reason this type of electrical activity, although contributing, is not the most relevant for the generation of the signal measured by EEG electrodes at scalp level. The other electrical behaviour which characterize the

neuronal activity is due to synaptic activity with which the neuron communicate and that is strongly related to different types of receptors involved in the process. Due to the presence of different receptors, the post-synaptic activity can induce both a positive (excitatory) or a negative (inhibitory) potential, thus inducing an inflow or outflow of extracellular current which tend to form a closed loop between sources and sinks of potential activity. This type of potential and induced current is slow and is known as Local Field Potential (LFP). The ensemble of synchronized neurons spiking over a large enough brain area makes possible to detect their activity at scalp level as a summation of LFP. Other than the previously described generative nature of electrical sources, the medium in which this signal propagates plays a crucial role on the possibility to effectively detect it via the exploitation of electrodes placed at scalp level. In particular the nature of different tissues characterized by different conductivity properties along with the geometry of the system can influence dramatically the quality and thus the feasibility itself of EEG signal acquisition. In fact two conditions must be present given which the LFP can be detected at scalp level and form the major constituent of the EEG signal. The first condition, as mentioned before, is that a large enough brain area must be activated coherently to generate a virtual dipole large enough to be detectable at scalp level, given the attenuation and filtering of the tissues and skull. The other condition is related to the geometric structure of the considered brain area. This area in fact must be suitable to position the aforementioned dipole in such a way it can generate a far field emission. The far field condition is necessary for the signal to be detectable and measurable by the electrodes of the EEG data acquisition system. Indeed each electrode works like a small antenna, which can work optimally in the far field conditions. This means that these electrodes can be essentially blind to source dipoles placed in wrong orientation. This is an intrinsic limitation with which electroencephalography must deal, given that the structure of the brain is folded and gyri and sulci represent its intrinsic geometric and structural nature. This means that, for example, if the patch of coherently activated neuronal population is placed in one position, such as in a sulcus, so that the representative dipole is tangential to the electrode directly placed above it, this electrode will see a zero mean activation, thus it will not be able to detect any relevant activation.

2.1.2 Measured signal

In the previous subsection we described briefly the nature of the electric signal EEG deals with. Here we consider the problem from a macroscopic perspective, presenting the properties of the EEG measured signal. At a scalp level the EEG signal is measured by a set of electrodes accurately placed on the subject's head. Each of these electrode measure a linear weighted summation of sources, as previously described, which come from the area directly placed under the electrode as likely as from more remote but strongly activated zones of the brain. This set of measurements, one for each electrode and at a rate established by the sampling rate (this can be of the order of 5000 Hz or higher) gives birth to the EEG signal which is thus formed by a spatial topography and associated time courses. Historically, given the high temporal resolution typical of EEG, the temporal measured signal has received great deal of attention in both its temporal and frequency domains. Recently also the spatial domain has been investigated with greater effort, putting the EEG techniques into the field of neuroimaging methods.

2.1.2.1 Temporal Domain

The easiest approach to the analysis of the measured EEG signal is to deal with its temporal characteristics. This means that given a set of trials (50-100) in which the subjects undergo the same stimulation it is possible to time-lock analyse the measured EEG signal via an average of the signal across trials. The result of this approach is called Evoked Related Potential (ERP). The obtained waveform can then be interpreted and further investigated both in terms of topography and of temporal characterization. In fact it is possible to identify a set of different behaviours described by the polarity of activation and their latency. This means that it is possible to make a nomenclature of all the dynamics of the signal by means of the polarity and cardinal position or latency in time (i.e. P1, P2, N1, N400 etc.). The latency of the dynamic is associated to the nature of the brain activity (sensory < 200 ms, higher level cognitive function > 250 ms).

2.1.2.2 Frequency Domain

Along with the characterization of the EEG signal in time it is possible to explore its properties in the frequency domain, especially considering dynamics and fluctuations

at different frequency bands. These oscillations have been extensively investigated in literature and each brain rhythm has been associated to different brain states. An important caveat in this analysis is that different phenomena could originate same frequency band oscillations. This means that different brain activity can reflect into similar frequency modulation. The nomenclature of these frequency bands is as follows: alfa(8-12 Hz), beta (15-30 Hz), gamma (>30 Hz), delta (<4 Hz) and theta (4-7 Hz) (Steriade and McCarley, 2005).

2.1.2.3 Spatial Domain

Due to the low spatial resolution of EEG signal the spatial domain received less attention till recent years. Recently the topography of scalp signal has been taken into account in data driven based techniques for data analysis, in particular Independent Component Analysis (ICA) and machine learning based methods such as clustering methods. In particular, under some constraints it has been possible to exploit those techniques to obtain unique spatial maps to further interpret or analyse. A practical example which received great deal of attention is that one related to the brain EEG microstates. Using spatial clustering techniques based on the measured topographical information it has been discovered the presence of quasi-stationary brain states which last shortly. These microstates are easily identifiable and can be related to organized brain activity. On the basis of these kinds of analyses the problem of source imaging can then be addressed more precisely, thus leading to real neuroimaging interpretation.

2.1.2.4 Inverse Problem

As mentioned before, it is possible to exploit the temporal, frequency and spatial information to infer knowledge about the brain structure and behaviour. However, in order to disentangle the sources of the signal and to come back to the microscopic level described in the generative model, it is necessary to reconstruct the sources which generated the actual signal. This problem is intrinsically ill-posed from an electromagnetic point of view, given that the same topography can be generated by an infinite distribution of currents. For this reason a bunch of constraints can be introduced, to limit the reconstruction only to meaningful source configurations. These constraints can come from *a priori* knowledge on the brain activity of interest (such as spatial location) and/or on a realistic model of the propagation tissues (i.e. with realistic modelling of

the subject head). Obviously other constraints can come even from other brain imaging modalities used concurrently or in parallel.

2.2 Functional Magnetic Resonance Imaging

In this section the fundamentals of fMRI signal are recalled briefly to permit the reader to get familiar with the origin of the signal and its main characteristics.

2.2.1 Source of the signal

In order to understand the properties of the fMRI signal it is necessary to address the issues related to the generation of it terms of both its relationships with the brain activity, and the physic behind the possibility of measuring this activity. The latter will be described in more details in the next subsection, while in the following we will describe the generative model associated to the fMRI signal. First of all, it is well known that the nature of fMRI signal is very different from that of EEG, since EEG reflects directly the activity of neurons via measuring their electrical behaviour, whereas fMRI is an indirect metric of this neuronal activity (Menon and Crottaz-Herbette, 2005; Mulert and Lemieux, 2009; Ullsperger and Debener, 2010). The electrical activity of neurons as measured by EEG is in fact symptom of underlying neuronal computation. In order to make possible this computation, neurons need adequate energy supply which is basically furnished by the blood flow. This means that the neuronal activity is able to drive the blood flow, and the fMRI signal is in fact related to the haemodynamic response to this neuronal activity. In nuce the activation of neuron imply oxygen consumption and synaptic transmission entails the elicitation of vasoactive signaling molecules and mechanism regulating vasodilation and constriction (as glutammatergic neurotransmitters). This mechanisms try to solve the need of oxygen of neurons which is in turn addressed by delivery of it via the modulated blood flow. This effect is known as Blood Oxygen Level Dependent (BOLD) response. The BOLD response results thus strictly related to neuronal activity, but it is intrinsically affected by other elements, such as the anatomy of capillary, vessels and veins distribution. Moreover the fact that this represents an indirect measure of neuronal activity modulated by the blood flow entails that the temporal resolution which can be reach is not due to the activity itself, but to the time the blood flow react to it delivering the oxygen. This is called

haemodynamic response and is typically of the order of 5-10 seconds, thus much higher than the millisecond resolution of electrical activity.

2.2.2 Measured signal

The entire fMRI technique is based upon the properties of the matter in interaction with magnetic fields. When placed in a magnetic field, protons (in this case protons of hydrogen) tend to align to the magnetic field itself, generating a magnetization vector whose magnitude depend on the strength of the magnetic field. In order to perturb this orientation it is then necessary to furnish a certain amount of energy, which can be transferred only at a certain frequency, called *Larmor frequecy*, which depends on the nature of protons and on the value of the magnetic field. This means that the energy transmitting system and the protons must be *in resonance*. Once perturbed protons tend to recover alignment with the magnetic field emitting a signal which can be finally measured and exploited. The BOLD related deoxyemoglobin works as an endogenous contrast agent within blood flow and volume, whose magnetic properties give birth to the measured fMRI signal.

2.2.2.1 Image Generation

As stated above, a perturbed proton in a magnetic field emits a signal while recovering its original position. This signal can be measured and used to infer the status of the proton. But in order to create an image it is necessary to encode spatial information in the detected signal. For this aim the MRI machines are provided with gradient magnetic field generators, which are added to the static magnetic field. Their use is to alter the *Larmor frequecy* so that different position in the brain will be described by different frequency and phase property. This permits to reconstruct a full image with a very high spatial resolution thus making of fMRI a very popular neuroimaging technique non invasive and suitable to address neuroscientific questions.

2.2.2.2 Image Contrast

As we have stated above, different tissues and matters are characterized by different *Larmor frequecy*. Thus it is possible to measure the signal emitted by different tissues in terms of decay of the longitudinal (T1 time constant) or transversal (T2 and

T2* time constants) components of the magnetization vector generated as described above. Mapping these temporal decays would permit to highlight different tissues, as it happens for the BOLD signal. In that case the presence of high concentration of oxygenated hemoglobin would reflect in higher T2*, whereas the opposite would reflect in lower T2*. In fMRI regions activated are thus brighter than those which are inactive.

2.3 EEG-fMRI

In this section we introduce the EEG-fMRI multimodal imaging, describing the principles and characteristics of this approach.

2.3.1 Advantages and challenges of simultaneous EEG-fMRI

When considering the properties of EEG and fMRI techniques it is immediately clear how they appear to be complementary in the nature of the signal they make available to the researcher. In fact, as mentioned before, the descriptive characteristic of EEG is that of noninvasively measuring the electrical activity of cortical neurons via electrodes placed on the scalp. This entails that EEG is able to follow fast dynamic of the signal with a temporal resolution down to milliseconds and less. On the other side, the relatively low number of electrodes and the nature of the inverse problem of source localization, which is intrinsically ill-posed, make it impossible for EEG to have an unique solution on the exact location of the sources of the signal, thus not permitting to the EEG technique to obtain a high spatial resolution of brain imaging. The properties of fMRI are the opposite. In fMRI the spatial localization of the signal sources is identifiable at millimetre scale, while the temporal resolution is blurred by the haemodynamic response function, which is related to the physiology of the measured signal and thus acts as a temporal low-pass filter lowing the temporal resolution to some seconds.

For these reasons researchers immediately found interest into the possibility of combining the two techniques into a multimodal imaging method, thus hoping to reach both high temporal and spatial resolutions (Debener et al., 2006, 2005). To reduce sources of experimental variability a big effort has been spent into the realization of a simultaneous EEG-fMRI acquisition framework. This framework presents several intrinsic problems and challenges due to the fact that both EEG and fMRI interfere with each

other. In particular, while effects of EEG onto fMRI data can be in first instance considered not too critical, fMRI environment is typically considered hostile for the EEG data acquisition system (Mulert and Lemieux, 2009).

Due to the Faraday's law a current is induced into conductors immersed in a variable magnetic field. Due to this, the wires of EEG cap which are placed into the strong static magnetic field, the gradient dynamic field and the RF signal of the fMRI, suffer for the presence of induced currents which alter the acquired signal with artefacts, making it difficult to measure and identify the brain signal of interest. For this reason advanced methods of artefact denoising must be implemented and adopted with the aim of obtaining a clear EEG signal acquired within an MR environment. In particular gradient and ballistocardiogram artefacts must be eliminated before performing any other kind of data analysis.

2.3.2 Safety Issues

The challenges of performing a simultaneous acquisition of EEG signal within the magnetic resonance environment translate directly into safety issues for the subject undergoing the acquisition. In simultaneous acquisition the factors of risk coming from canonical EEG and fMRI signal acquisition are summed up and new risks come from the combination of the two. In fact the sources of noise presented in the previous subsection, i.e. the presence of induced currents in the EEG system, not only reflect in the quality of the signal, but, much more critical, they reflect in direct risks for the subject. In particular, the main general issue is that the presence of time-varying field induced currents could generate an amount of heat of electrodes which can cause burns to subject's tissues in contact with them (Angelone et al., 2004; Laufs et al., 2008). It is relevant to note that different fMRI acquisition sequences (like Fast Spin Echo) generate different amount of induced current and thus of heating on the EEG electrodes (Mulert and Lemieux, 2009). Many different solutions can be implemented in order to reduce the risk of over-heating and manufacturers offer fully MR-compatible EEG systems which take into account these solutions.

2.3.3 Data Fusion

The last section of this chapter is devoted to briefly describe the methods implemented in the state of the art of multimodal data fusion. When dealing with data fusion of

EEG and fMRI signals it is possible to classify the methods proposed in literature into two main groups, i) those which consider more relevant (and thus as independent) one data type while considering dependent the other one and ii) those which exploit the two data sources giving them the same weight. The first type of methods are those firstly developed and typically implemented with univariate model-driven algorithms such as regression. These methods are those which use the EEG time course as a regressor to predict the fMRI activations (Lemieux et al., 2007) or exploit the fMRI spatial maps as a constraint for the localization of EEG dipoles in the inverse problem solution (Phillips et al., 2002).

A more fascinating approach is the more recent one, which can be considered as a true data fusion since it fully exploits the information content present in the two datasets considering the two data sources as independent variables to be jointly analysed. The methods that follow this approach are mainly based on multivariate data analysis algorithms and are often data driven instead of model driven, thus making little (or none) arbitrary assumptions on the underlying nature of the data themselves. For an exhaustive review of multivariate methods for multimodal data fusion the reader is referred to (Sui et al., 2010). The most interesting methods proposed in the literature are those based on Independent Component Analysis (ICA), Partial Least Square (PLS) and Canonical Correlation Analysis (CCA). ICA can be applied in different ways, that is jointly or in parallel. Applying jointly ICA means that the data or the features extracted from the data are concatenated and then ICA components are related to both data sources. The parallel ICA computation keeps the two datasets separated and integrates the results via constraining the two unmixing matrices to be maximally correlated. These methods are fully exploratory and extract meta-information in terms of Independent Components (IC) that describe some common behaviours which are statistically meaningful. CCA permits to each dataset to have different mixing profiles while keeping components associated between the two datasets. This method permits different datasets to be decomposed with minimum constraints maximizing covariation across the two data sets. Finally PLS is an interesting hybrid method between exploratory and hypothesis based. It decomposes the two dataset in such a way that a link is established between a set of hidden factors (i.e. predictors) called latent variables and the dataset itself (i.e. dependent variables). When keeping the latent

variables equal for different datasets, the associated components into each dataset will be linked through the common latent variables themselves.

3

Real-time Neuroscience

3.1 Rationale and Principles

Soon after the methods of measuring brain activity have been discovered and developed, the intriguing possibility of analysing and exploiting brain signal in real-time, that is during their ongoing generation and evolution, became topic of great interest due to the vast amount of possibilities and applications related to it. Researchers soon discovered that the exploitation of brain signal would have open a new channel previously unknown, opening the doors to new research modalities as well as practical applications in both clinical and everyday life. A general real-time system is constituted of three main parts, a data acquisition system (i.e. the neuroimaging technique), a data analysis system (i.e. the algorithms and mathematical methods used to obtain the relevant signal from the data) and a signal exploitation system (i.e. , depending on the application, the feature translation system for BCI or for neurofeedback).

The usual goal of a real-time system is to permit the identification and monitoring of an activity of interest during its ongoing development and actuation. The identification is defined as an initialization phase where the real-time analysis and derived spatial-temporal features to be monitored are defined, usually with a functional localizer (FL) or a classification training step (LaConte et al., 2007). The monitoring represents the execution of the on-line analysis of the event of interest and the real-time delivery of results that can eventually operate on the stimulation paradigm. From a conceptual point of view, it is thus possible to discriminate the identification and monitoring phases and to develop different algorithms and strategies to deal with them.

3.2 EEG

Historically the most adopted neuroimaging technique to implement real-time system has been EEG due to its intrinsic low cost, portability and high temporal resolution. The approach is usually to exploit the set-up in order to make BCI systems. The brain signal is thus extracted and associated to different commands, making it possible to control a device. During the years different criteria have been exploited in order to build a robust system. The most interesting and basic aspects of a system are related to the type of brain signal exploited and the type of algorithm adopted to analyse the signal. In fact, depending on the target of the real-time application, it is possible to use different brain properties or behaviours.

3.2.1 Type of brain signals

Two different issues are the underlying mental state and the brain signal used in the application. This means that for example in BCI application the command signal to control a device can be of any kind as long as it is a stable and easily identifiable electrical brain signal. Since the brain responds with electrical signals to stimuli of very different nature it is possible to try a classification of these kind of responses. A working classification of the brain responses can be to discriminate between internally and externally triggered brain signals (Cichocki et al., 2008). Internally triggered signals are brain activations which are endogenous to the subject, i.e. that the subject autonomously decide to instantiate. An example of this kind of signals is motor imagery, which is arbitrarily controlled by the subject. The other type of signals are the externally triggered. In this case the brain state modulation is induced by external stimuli. This is for example the case of the famous P300 speller, in which the P300 signal is triggered by an external visual flashing device. The subject in this configuration does not have the direct control over the P300, but he uses the device to generate it. Along with this different nature of brain signal it is worth noting that different features can be extracted to increase the signal to noise ratio of the representation of the signal. For example the imagined motor activity can be internally triggered and then detected extracting as a feature the *Mu* rhythm, whose reduction or de-synchronization is known to be related to the motor planning and execution. Different approach to extract another feature could be obtained by applying ICA to extract the independent components

(IC) associated to motor activity in terms of topography or temporal behaviour. In this case the feature would be an IC of interest instead of a frequency rhythm. Once the features have been extracted, another critical step is the classification to detect the presence (or the modulation) of the behaviour of interest to permit the BCI control. In the next section a brief summary of main algorithms adopted in real-time EEG will be presented for both feature extraction and classification.

3.2.2 Algorithms used in real-time EEG

Many of algorithms have been used to implement the data analysis step in EEG based real-time systems (Bashashati et al., 2007). A huge amount of advanced techniques mutuated from the signal processing field have been adapted in order to extract and classify the behaviour of interest from the brain. Several classification methods have shown to be suitable for BCI systems leading to robust and high performing set-ups. These classification algorithms cover the state of the art knowledge starting from simple threshold detectors to advanced Support Vector Machine or Neural-Networks based classifiers. An extensive description of these methods is out of the scope of the present thesis. The reader is referred to (Bashashati et al., 2007) for an exhaustive review over data processing techniques adopted in BCI systems.

3.3 fMRI

3.3.1 ICA for real-time fMRI

Real-time fMRI (rt-fMRI) is an emerging neuroimaging tool based on the estimation of brain activity in real time (typically around 1-2 seconds) (deCharms, 2008; LaConte, 2011; Weiskopf et al., 2004b, 2007). This tool can be used not only for overall monitoring of fMRI data quality (Weiskopf et al., 2007) but also for manipulating the cognitive state of the subject based on its own brain's activity (Shibata et al., 2011). This neurofeedback approach has been used in various fields of cognitive neuroscience such as attention (Thompson et al., 2009) and emotion (Posse et al., 2003). Neurofeedback approaches have also been used with rt-fMRI in clinical research, such as the study of control of chronic pain (deCharms et al., 2005) and the control of craving.

Since its advent real-time fMRI has had to face a number of technical challenges, mainly due to the computational load of the data analysis, which directly competed

against the goal of providing real-time feedback (i.e. < 1 TR). However, recent technological advancements provide a way to overcome this issue making large scale computations possible even on standard platforms (Weiskopf, 2011; Weiskopf et al., 2007). These technical advances enable us to shift our focus of attention from technical issues to data analysis aspects.

Considering data analysis techniques, the initial and still most common analysis framework for rt-fMRI has been based on univariate hypothesis-driven approaches, with adaptation of standard algorithms, such as the general linear model family (GLM), to the real-time domain (Cox et al., 1995; Gembris et al., 2000; Hinds et al., 2011). These methods are common mostly because they are associated with easy interpretability and fast computation. In these approaches both the identification and monitoring phases are typically implemented using hemodynamic response-based models of the expected cognitive tasks and eventual nuisance variables taking place during the rt-fMRI experiment.

Another family of data analysis techniques is represented by the multivariate data driven algorithms, which have shown a great capability of exploiting the full information content intrinsically present in the data to be analysed without assuming the explicit shape or timing of the hemodynamic response to a stimulus (McKeown et al., 1998; Mouro-Miranda et al., 2005; Norman et al., 2006). The driving motivation behind these methods is that they allow characterizing functions that may not be detectable without exploiting both second order (variance) and higher-order statistics, thus relying on a greater amount of information. These properties make the multivariate data-driven techniques very appealing for use in the real-time domain. Within this concept several machine learning algorithms have been successfully adopted and exploited in the real-time data analysis framework. The most successful implementations have been those based on support vector machines (SVM) (LaConte et al., 2007; Magland et al., 2011; Sitaram et al., 2011). SVM provide a powerful solution to a number of applications that are subject specific, at the cost of training the classifier and imposing some interpretability issues on the results. In this context, the two phases of the canonical rt-fMRI framework are represented by the two steps of a classifier, i.e. the first phase is the training of the classifier, and the second phase is the test or execution of the classifier (i.e. the classification itself).

In addition to SVM, independent component analysis (ICA), another multivariate data driven technique, has proven to be very effective in fully exploiting the complete amount of information which is present in the data. ICA enables the extraction of knowledge other than that merely modelled in a classical univariate approach (Beckmann and Smith, 2004; Calhoun et al., 2001; Hyvrinen and Oja, 2000). Furthermore, ICA methods can also be applied in a series of problems for which univariate inference cannot offer a solution, i.e. in experiments that lack a regressor model to be adopted in the univariate analysis. This is the case for resting data analysis or also experiments with particular patient populations (Calhoun et al., 2009).

Independent component analysis (ICA) is a data-driven blind source separation (BSS) method widely used in brain functional magnetic resonance imaging (fMRI) data analysis (Calhoun and Adali, 2006; McKeown et al., 1998). The basic idea underlying ICA is to disentangle in a multivariate way all independent components (ICs) whose combination gives the actual measured signal. The generic procedure is thus to fix an arbitrary number of ICs, i.e. the model order, and let the algorithm exploit a criterion of independence to compute the decomposition that optimizes the criterion given that model order. Several algorithms have been proposed to measure independence of the sources in order to separate them into ICs. The most popular criteria have been based on information theory principles, such as the Infomax algorithm (Bell and Sejnowski, 1995) or higher order statistics (second, third and fourth order cumulants), such as kurtosis fastICA (Hyvrinen and Oja, 2000). Given the nature of data-driven BSS algorithms which try to deal with, and take advantage of, an enormous amount of data, ICA found an optimal field of application in the analysis of fMRI data. Its canonical use has been that of analysing data in off-line fashion, that is, once all experimental data has been already acquired. In the perspective of this paper the use of ICA off-line can be defined as analysing data in well-posed conditions, as we have usually a great amount of time available for computation and an entire dataset with all the relevant information in it.

A very different situation arises if ICA is to be considered for dynamic studies such as real-time fMRI (rt-fMRI), in which there is an interest in the dynamic characterization of brain states during the experiment (deCharms, 2008; Weiskopf, 2011). ICA methods could be of interest in such studies for their data-driven nature, particularly when considering experimental designs in which hemodynamic response models will be

difficult to use for predicting the brain states under investigation, such as resting state. In a real-time fMRI context ICA will work under ill-posed conditions because the data needs to be analysed under critical time constraints and with a reduced dataset. In addition, since the data changes dynamically whereas the algorithm is usually fixed, the choice of the algorithm can drastically affect computation time and quality of the results.

The idea of translating ICA properties to a real-time implementation was firstly proposed in a seminal paper Esposito et al. (2003) and implemented as a plug-in in Turbo Brain Voyager software Goebel (2012). In this initial work the authors presented a FastICA based rt-fMRI analysis tool exploiting precise design choices and including an identification phase and a monitoring phase. The first identification phase solved the problem of ranking ICs of interest, i.e. a canonical univariate functional localizer step was implemented to define areas of interest. Other ways to solve the problem of ICs ranking could be represented by exploitation of expected characteristic feature of the ICs of interest via a classifier DeMartino et al. (2007). The second monitoring phase used on-line execution of FastICA (implemented in a sliding window fashion), for extracting different ICs. The ICs were ordered on the basis of their spatial overlap with the IC of interest, which in this case consisted of single-slice representation of motor activity derived from a finger tapping localizer.

This first approach to the implementation of ICA algorithms for real-time fMRI demonstrated that the fastICA algorithm can be successfully used in such a problem. This study gave two main results. Firstly, it demonstrated on both real and simulated data that the expected task-related activity was equally detected by ICA and the standard general linear model (GLM) approach. Secondly, ICA was able to detect transient or unexpected neural activity which had not been originally included in the haemodynamic response model. These results support the motivation of the evaluation and use of ICA in a real-time fMRI experiments.

3.3.2 ICA mathematical preliminaries

Since all the methods presented in *Chapter 5* and *6* share a common core based on ICA principles, we briefly recall the main mathematical concept associated with the ICA. Let's assume that we have a set of fMRI measurements Y_i where $i = 1, ..., v$ is the index of voxels and each Y_i is a vector of y_{ij} elements, where $j = 1, ..., t$ is the index of

time points. The entire dataset can thus be represented as a matrix Y of dimensions time points by voxels. Now, let's assume that the signal measured in the dataset is generated by a subset of n underlying sources which are linearly mixed and summed up. This reflects in the following canonical formulation using the vector-matrix notation

$$Y = AX \tag{3.1}$$

where Y is the acquired data matrix of dimension equal to the number of time points by the number of voxels, A is the mixing matrix of dimension equal to the number of time points by the number of sources to be recovered and X is the matrix of the sources (i.e., ICs) of dimension the number of sources by the number of voxels. Each j^{th} row of Y is a vector $y_{ji=1:v}$ represents an fMRI volume in a j^{th} time point and is thus obtained by the linear weighted combination of hidden sources spatial maps $y_j = a_{j1}x_1 + ... + a_{jn}x_n \forall j$. This means:

$$Y = \sum_{j=1}^{n} a_j x_j \tag{3.2}$$

Given this definition and assuming that the sources x_n are mutually independent, it is possible to recover those hidden sources by computing an estimation of the unmixing matrix $W = A^{-1}$ such that:

$$X = WY \tag{3.3}$$

is an estimate of the sources. The estimation of W can be obtained via different algorithms, leading to different ICA implementations with different properties and effectiveness. See (Bell and Sejnowski, 1995) for details. The FastICA algorithm (Hyvrinen and Oja, 2000) exploits the non gaussianity as a metric of independence of the sources. This means, in the simplified iterative algorithm for several units, that the estimation of W is obtained through the following steps

1. Initialize randomly W
2. Given $W = \frac{W}{\sqrt{\|WW^T\|}}$
3. Repeat until convergence $W = \frac{2}{3}W - \frac{1}{2}WW^TW$ and step 1-3

Other approximations of the solution can be obtained, but a detailed description of the methods to obtain FastICA decomposition is anyway out of the scope of the present chapter.

4

Experiment 1: Design of a real-time framework for fMRI and EEG experiments

4.1 Introduction

This chapter describes the hardware and software system set-up which has been used to test the real-time methods developed during the PhD thesis and presented in the following chapters. The realization of this set-up has been part of the thesis and required a considerable amount of time and resources of the PhD itself, since several solutions have been implemented and tested. The problem of developing a running real-time system poses several issues and problems that must be solved. The solutions to develop include the data acquisition step, the data analysis step and the stimuli delivery step. In the state of the art systems for real-time analysis (Goebel, 2012; LaConte et al., 2007; Weiskopf et al., 2007; Zotev et al., 2012). These three steps are done by three different computers which communicate with each other, the data acquisition (i.e. the control of the scanner) is ruled by one computer, the data analysis by another one and finally the stimuli delivery is controlled by a third computer. All these computers must be able to share connections in order to make it possible to run an experiment with the minimum delay between the stimulus delivery and the acquisition of the corresponding signal response. In the following, each of the three steps will be described separately, along with the proposed implemented solutions. Figure 4.1 represents a scheme of how

the system architecture is defined in our facility. Actually, as it will be described in the last section, only the data flux of fMRI acquisition is practically built. The EEG part has been tested only off-line.

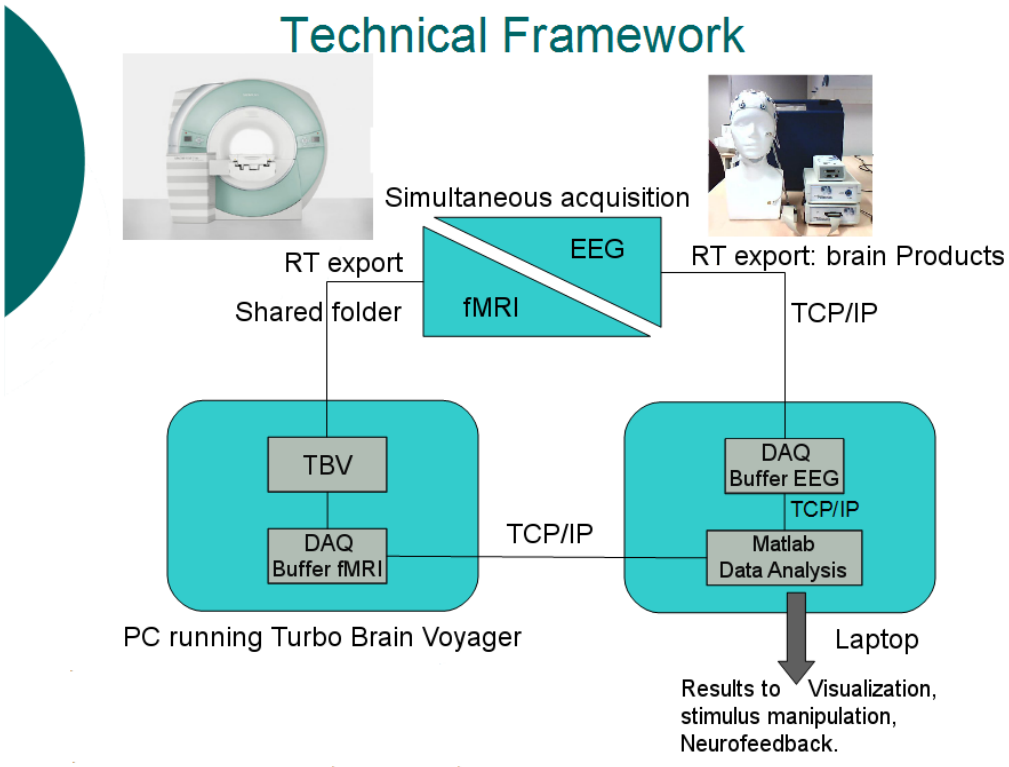

Figure 4.1: Experiment 1- Schematic Description of real-time EEG-fMRI Hardware and Software Set-up - In this figure a scheme of the adopted set-up is reported. It is highlighted the flux of data and information from both EEG and fMRI subsystems, along with the location of the software subsystems for data analysis and visualization. TBV is the Turbo Brain Voyager software, DAQ is the data acquisition buffer used by matlab to mimicry multi-threading.

4.2 Data Acquisition

fMRI data are acquired by a 4T Bruker scanner, controlled by a Siemens software. The export of the data is realized through coding a modified acquisition sequence (Weiskopf et al., 2005, 2004a) which permits to split the flux of the acquired volumes and save

them jointly in the system and in a shared folder while they are acquired (i.e. volume by volume). This sequence has been slightly modified in order to export data corrected for inhomogeneities of the magnetic field using the Point Spread Function (Zaitsev et al., 2004). From the shared folder the data will be made available to external computers. It is worth noting that the new versions of Siemens control software makes it possible to easily export the data as an intrinsically implemented feature of the software by enabling an option.

4.3 Data Analysis

After the collection of the data into a shared folder, the data analysis software need to be developed. As a successful first pilot experiment using Turbo Brain Voyager (Goebel, 2012), we found necessary to develop an independent system in order to make it possible to have a full control over all the details of the analysis. A first approach has been to develop it on a laptop with linux-based environment in c++ using state-of-the-art libraries for data transfer and analysis. Due to problems related to the portability of the system and compatibility with the Windows-based environment of the scanner computer, another solution fully Matlab based has been implemented and tested. The use of Matlab software made it necessary the exploitation of several solutions, since Matlab is intrinsically a single-threaded application. This means that several threads cannot be activated in parallel, i.e. while one operation is ongoing another one cannot be started. In other words, if new data arrive while Matlab is computing something, these new data will be lost. For this reason a buffer developed by FieldTrip `http://fieldtrip.fcdonders.nl/` was included and adapted in the development, in order to make it possible to keep memory of the data while processing the signal. All the rest of the code has been in-house developed exploiting ICA algorithm implementations as available from the Matlab-based package GIFT `http://mialab.mrn.org/software/gift/index.html#`. The implemented data analysis methods will be described in *Chapter 6*.

4.4 Stimulus Delivery

The stimulus delivery system has been implemented in Matlab exploiting an adapted version of Tools for NIfTI and ANALYZE image by Jimmy Shen `http://www.mathworks.com/matlabcentral/fileexchange/8797`. This tool has been used to deliver to the subject the spatial map of his brain activation detected by the data analysis techniques developed. Along with the spatial map, even the associated time course can be send to the subject in different formats, such as a bar whose magnitude is adapted to the level of activations or as an ongoing graph. This visual stimulus delivery is obtained by starting a parallel Matlab session on the same computer as the data analysis is ongoing. This new Matlab session is located on a secondary screen of the computer, which will be shown to the subject within the scanner.

4.5 Limitations

It is worth noting that some limitations are present in terms of the extension of tests performed on the presented framework. In particular the flux of fMRI acquisition (left part of Figure 4.1) has been tested with phantom sessions and pilot sessions, while the flux of EEG acquisition (right part of Figure 4.1) has been tested with simulating real-time experiments using previously acquired EEG data, but exploiting the same software set-up as the one adopted within the scanner environment.

5

Experiment 2: Selecting ICA algorithms and parameters for real-time fMRI applications

5.1 Introduction

As presented in the introduction, the use of advanced BSS algorithms in real-time fMRI is very promising for the further development of the method and for the practical exploitation of it behind the proof-of-concept theoretical level. One of the most investigated BSS method in literature is ICA, which has been successfully applied in several off-line fMRI data analysis experiments. However, there are many possible choices for ICA algorithms, differing mostly in the mathematical criteria used to establish source independence, and it is not obvious which of these algorithms could best characterize neural activity as captured by the BOLD contrast. Besides which particular algorithm is used, there is also freedom for the parameter settings and it is not clear how these could affect the performance of an ICA-based rt-fMRI analysis. Indeed, performance comparisons among different ICA algorithms applied to fMRI data have historically been reported only for the well-posed off-line fMRI case in which the full acquired time-series data is available after the experiment (Correa et al., 2007, 2005; Esposito et al., 2002). Further, from off-line ICA experiments it is known that *a priori* conditions may help the identification of a particular IC most congruent with a predefined target, such as a spatial map (Lin et al., 2010). This *a priori* knowledge can be im-

plemented in different ways depending on the characteristics of the algorithms. It can be as low invasive as a simple tailoring in the nature of the statistical distribution to be extracted, i.e. weighting more super-gaussian or sub-gaussian distributions, or as constrained as targeting a specific timecourse or spatial map. This approach is known as semi-blind decomposition, and its main property is to fuse the positive principles of data-driven algorithms with some kind of *a priori* knowledge on the problem of interest. The introduction of *a priori* knowledge can be done in several ways, e.g. by orienting the decomposition of data into sources with some specific properties. An example of a semi-blind approach is presented in (Lin et al., 2010), in which a spatial *a priori* constraint is introduced in the decomposition algorithm with the aim of extracting the source most congruent with a predefined spatial target. The motivation of considering priors include reduced computational time (as *a priori* information suggests short cuts in the decomposition to the algorithm), and improved quality of the sources obtained (given that the results are closer to what is expected). In general not all ICA implementations foresee the possibility of introducing prior knowledge at spatial or temporal level. In this context, and given the noisy data of rt-fMRI experiments from the limited data available for analysis, it is of interest to extend the evaluation of real-time ICA strategies with the consideration of temporal and spatial priors.

In this chapter we investigate and compare the performance of various ICA algorithms under the ill-posed conditions imposed by real-time fMRI. We use fMRI data of healthy subjects performing a visual-motor task in a framework that simulates a real-time acquisition for each subject separately. Four brain networks were extracted in each subject from the full time course and used as target networks for the performance evaluations when using only a part of the time series: the right and left visual motor networks, the default mode network, and a noise network associated with physiological noise. In each network we tested 14 different publicly available ICA algorithms, and for each we investigated how the length of the time window (i.e. the number of time points) used for the analysis, the model order (i.e. the number of computed ICs) and the type of *a priori* information (none, spatial or temporal) affect performance. The evaluation of performance was done by considering computation time together with the spatial and temporal correlations of the dynamic ICs with the network reference target. The goal was thus to find, for each network, the ICA implementation that gave the fastest and highest spatial and temporal similarity to the target, but using only a

fraction of the time series. The obtained results will be the base for the implementation of novel ICA-based method presented in the next chapter.

5.2 Materials and Methods

We refer the reader to the Appendix for details on the acquisition paradigm for the fMRI dataset adopted in the analysis performed in both Chapter 4 and 5.

5.2.1 ICA Algorithms

A total of 14 different ICA algorithms were considered (see Table 5.1). The algorithms were available from the GIFT toolbox and most of them were discussed in a recent comparative study (Correa et al., 2005). The list includes algorithms already used in real-time fMRI experiments, like the fastICA algorithm (Esposito et al., 2003). These algorithms, which are public and were taken as in their original distributions, differ in their data reduction preprocessing steps (e.g., centering, whitening, dimensionality reduction) and independence criteria for source separation (e.g., minimization of mutual information, maximization of non-Gaussianity) (Cichocki and Amari, 2002).

5.2.2 Parameters Analysed in the ICA Simulations

The main purpose of this real-time fMRI simulation study is to investigate a number of ICA algorithms to find the one that performs best across subjects using a trade-off of the following parameters:

1. Window length (i.e time length of data acquisition).

2. Model order (i.e. number of ICs).

3. Type of *a priori* information (none, spatial or temporal).

The choices for these parameters are discussed in more details in the following sections.

ICA Algorithm	A Priori Knowledge	Arbitrary Number of ICs
Infomax	yes	yes
fastICA	yes	yes
ERICA	no	yes
SIMBEC	no	yes
EVD	no	yes
JADEOPAC	no	no
AMUSE	no	no
SDD ICA	no	no
Semi-Blind Infomax	yes	yes
Constrained ICA	yes	no
Radical ICA	no	no
COMBI	no	no
ICA-EBM	no	yes
FBSS	yes	no

Table 5.1: ICA Algorithms - List of tested ICA algorithms and their possibility to accept as parameters arbitrary *a priori* knowledge (both Spatial and Temporal) and a varying number of ICs. Those algorithms which cannot accept an arbitrary number of ICs extract a numer of ICs equal to the time window length. These algorithms references are contained in GIFT toolbox (GIFT: `http://mialab.mrn.org/software/gift/index.html`).

5.2.3 Window Length and Model Order

The amount of data that an ICA algorithm uses depends directly on the number of brain volumes available in the growing time window, which in turn defines a limit to the maximum number of ICs that may be computed. In this study we focus on a growing window approach because were interested in finding an optimal window length. As the time window length becomes longer there may be a more accurate representation of the averaged dynamic responses of the brain because more data is available. However, this may come at the cost related to both reduce temporal resolution of the dynamics characterized and increase the computation time. Conversely, with shorter windows the characterizations may be faster yet less accurate. For the simulation of each ICA algorithm the window length was varied between 3 and 35 brain volumes (the full time series consisted of 220 brain volumes, and 35 TRs was approximate to the known period of the visual-motor tasks). For each time window length the number of ICs was varied between 2 (minimum meaningful value of model order in BSS) and the actual window length. Moreover, since for computational reasons the model order must be less than or equal to the window length, the window length minimum value has been set to 3. Thus while increasing the window length all possible model orders between 2 and window length were evaluated to find the best performing pair of parameters (window length and model order). Not all the ICA algorithms considered permit an arbitrary selection of the number of desired ICs. Some of them (jade-opac, amuse, Radical ICA, combi, ICA-ebm, FBSS) allow the possibility to extract only a number of ICs that is fixed for each run and is equal to the number of available data points. In our case, this means that for these algorithms the spanned parameter space will be represented by a line identified by the points in the space with equal number of ICs and time window length.

5.2.4 Use of *A Priori* Information

As previously mentioned, the exploitation of *a priori* knowledge permits an improvement in the performance of analysis which run in ill-posed conditions. However, it is worth noting that the use of *a priori* knowledge can also address another practical challenge of ICA decomposition, which is particularly relevant in ill-posed conditions. In fact a critical choice in ICA algorithms implementation is the ranking or selection of ICs. A practical challenge is to select and track the ICs of interest despite the

other ones. To address this problem the concept of either spatial (Lin et al., 2010) or temporal (Esposito et al., 2003) *a priori* information has been explored in literature. Other ways to solve the problem of ICs ranking could be represented by exploitation of characteristic expected feature of the ICs of interest via a classifier (DeMartino et al., 2007).

In the context of real-time fMRI, *a priori* information may be available from a localizer scan that elicits aspects of activation that are then to be tracked dynamically in a subsequent experiment. The priors can make the mathematical computation of ICA easier, driving the algorithm initial conditions closer to the basin of attraction of the target IC. In this simulation study the temporal and spatial IC priors were determined from the ICA analysis of the full timeseries. This *a priori* information is incorporated into the ICA algorithms as an initial estimation of the weighted matrix or as a final constraint of the shapes of the target IC. Due to the intrinsic characteristics of the ICA algorithms, only a subset of them allows us to incorporate spatial and/or temporal *a priori* knowledge in the analysis (see Table 5.1).

Given the general model of ICA (Calhoun et al., 2001), it is possible to describe an fMRI ICA problem as $\mathbf{Y} = \mathbf{AX}$, where $\mathbf{Y}$ is the data matrix of dimension equal to the number of time points by the number of voxels; $\mathbf{A}$ is a mixing matrix of dimension equal to the number of time points by the number of ICs; $\mathbf{X}$ is the matrix of the sources of dimension equal ti the number of ICs by the number of voxels. If we denote with $\mathbf{W} = \mathbf{A^{-1}}$ the weighting matrix (i.e. unmixing matrix), it is then possible to insert *a priori* information in the rows of the matrix $\mathbf{W}$ directly, if the information is temporal (i.e. a time course). In case the expected or known behavior is spatial (i.e. spatial map) it is possible to construct the $\mathbf{W}$ matrix as $\mathbf{W} = \mathbf{Y}pinv\mathbf{X}$ where that the rows of $\mathbf{X}$, i.e. the expected spatial maps of the independent sources are known and *pinv* is the *pseudoinverse* function. In one case (spatially constrained ICA algorithm (Lin et al., 2010)) the *a priori* knowledge is not given as initialization of the weighted matrix but, following the implementation, it has been imposed as final target of the decomposition. In this last case instead starting from a point close to the basin of attraction, the constraint means that the ending point will be close to the basin of attraction.

5.2.5 Computation of template ICs for performance evaluations

Four template ICs were identified on each subject by applying the Infomax ICA algorithm with 20 components to the full timeseries. The spatial maps and associated time courses of these networks were later used as reference and *a priori* knowledge options for the performance evaluation of different ICA implementations, in particular shorter time series to simulate real-time fMRI conditions.

The task-related networks were the right visuo-motor task (RVMT) and left visuo-motor task (LVMT), which were selected by visual inspection using as reference the originally published results (Calhoun et al., 2003). In addition, the default mode network (DMN) and a noise (NOISE) network were also identified and used as templates for networks typically present in resting state studies (Robinson et al., 2009; Soldati et al., 2009). Figure 5.1 shows sample spatial representations of the four template networks in a subject.

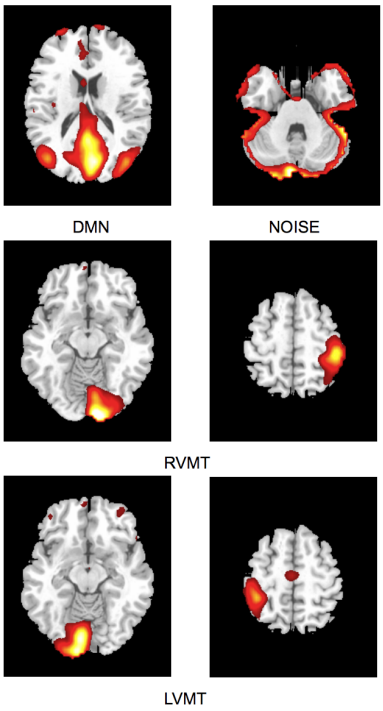

Figure 5.1: Experiment 2- Investigated brain activations - Spatial maps of ICs considered in the simulation obtained from Group ICA 20 ICs. For ease of visualization only the relevant slices are reported here. First row depicts Default Mode Network (DMN) and residual motion artifact (Noise). Second and third rows depict the two task related ICs, Right Visuo-Motor Task (RVMT) and Left Visuo-Motor Task (LVMT).

5.2.6 Evaluation of performance for different ICA implementations

The performance of each ICA algorigthm was assessed separately for each subject and network (RVMT, LVMT, DMN, NOISE) by systematically sampling the space of algorithm variables, finding for each variable set the target network ICs and comparing them with the corresponding template networks.

The ICA implementations for each subject and network were manipulated through the following variables:

- *ICA algorithm*: 14 algorithms listed in Table 5.1.
- *Prior*: all 14 algorithms were tested without priors. A subgroup of four algorithms (Fast ICA, Constrained ICA, ICA-EBM, FBSS) allowed the additional implementation of either spatial or temporal priors taken from the template ICs.
- *Window length (WL)*: for each algorithm the window length varied from 3 TRs to 35 TRs in a growing window scheme. The lower limit of 3 TRs was chosen as the minimum time course length for which an ICA can be computed. The upper limit of 35 TRs was chosen because it is approximate to the period of the cognitive task.
- *Model Order (MO)*: for each WL the model order was varied between 2 and WL.

These parameters were manipulated according to an iterative automatic procedure (Soldati et al., 2012), as schematically shown in Figure 5.2. Overall this meant that for each subject (a total of 3), network (a total of 4) and ICA algorithm (a total of 22: 14 with no priors, 4 with spatial and 4 with temporal priors), a total of 561 ICA computations were made (33x34, given 33 WL values and for each WL-1 possible MO choices). At each iteration the extracted IC results were compared with the templates to estimate the performance of the iteration's parameters.

The performance of each algorithm was characterized from the following three parameters:

1. *Spatial similarity with template network*: The target network IC was selected automatically by choosing the one with the highest spatial similarity (i.e. spatial

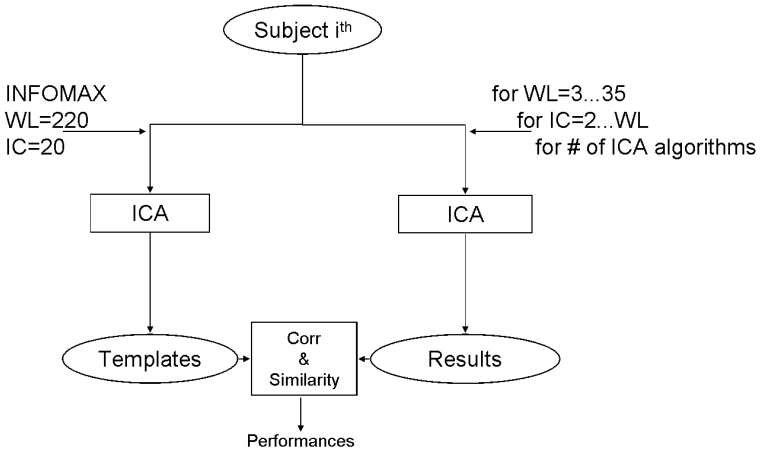

Figure 5.2: Experiment 2- Scheme of the procedure for testing ICA algorithms - Diagram of adopted method for ICA algorithm comparison. For each subject data are exploited for creating templates using INFOMAX with model order (ICs) of 20 and window length (WL) equal to the entire available time course. The ICA algorithms are then tested iteratively for each combination of IC and WL. Results of each computation are compared with templates and evaluated in terms of spatial similarity and temporal correlation.

overlap) between the ICs extracted and the template IC for the corresponding network. The spatial similarity metric was computed as the absolute value of

$$Similarity = \frac{a * b}{norm(a) * norm(b)} \tag{5.1}$$

where a and b are the vectors representing the spatial map (reshaped to 1D) of extracted and the template IC of interest respectively.

2. *Temporal correlation with template network*: The temporal correlation between the IC extracted and the template IC derived was computed, with its statistical significance (p-value < 0.05).

3. *Computation time*: The computation time to extract the ICs was recorded. Algorithms which gave computation times larger than the maximum WL (35 TRs, or 200s) were discarded. This threshold has been heuristically chosen to restrict the simulation to practical real-time fMRI implementations

Considering a fixed subject, brain network and ICA algorithm (with or without prior), the best performing ICA implementation (choice of WL and MO) was considered the one that gave the highest spatial similarity with a significant temporal correlation to the reference network and a computational time below the 200s threshold.

5.3 Results

This study evaluates the performance of different ICA algorithms in a real-time fMRI simulation that uses public fMRI data (Calhoun et al., 2003). The performance of various real-time ICA implementations is characterized on three task activated networks (motor, visual and default mode) and an IC representative of noise using three metrics: spatial and temporal similarity with the reference networks derived from the full fMRI time series as well as computational time (see Figure 5.3). The following variables were systematically manipulated in the various ICA implementations using a growing window approach: ICA algorithm, time window length, model order, use of spatial, temporal or no prior information. The goal was to find the implementations that would give the best compromise between highest similarity between the detected IC and the reference IC at minimal computation time. Figure 5.3 shows an example (mean over subjects) of the search for optimal combination of parameters in a sample network (right visual-motor cortex) when using one of the ICA algorithms (EVD). For illustration purposes, the growing explored space of window lengths (horizontal axis) and model orders (vertical axis) is sampled incrementally by seven areas covering different ranges of WL (MO is always from 2 to WL-1). For each of the sampled areas the optimal point is shown with its relevant information listed on the table in the figure. The figure shows how, for a fixed network and algorithm, the optimal performance can fluctuate depending on the amount of data available (window length) and the model order chosen. In particular, it can be seen that the optimal performance in different parts of the space is not given by the highest model order for a given window length.

Table 5.2 reports, for each of the networks investigated, the group performance results obtained with each of the ICA algorithms tested when no *a priori* information was used. The table shows mean results for the maximum spatial similarity (group standard deviation in brackets), corresponding computation time, growing window length and model order. For clarity, the values reported are only those for which the computation

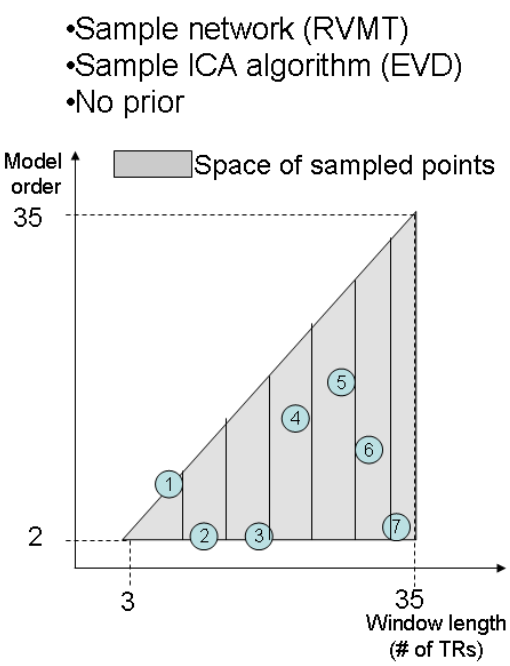

n	WL Range	Optimal WL	MO	SS	TC	CT
1	3-5	5	5	0.26	0.93	0.11
2	3-10	10	2	0.48	0.98	0.04
3	3-15	15	2	0.53	0.98	0.03
4	3-20	16	10	0.54	0.98	0.06
5	3-25	25	12	0.57	0.95	0.07
6	3-30	27	6	0.64	0.91	0.05
7	3-35	31	3	0.58	0.89	0.04

WL: window length
MO: model order
SS: spatial similarity with reference
TC: temporal correlation to reference
CT: computation time
RVMT: Right Visual Motor

Figure 5.3: Experiment 2- Example of results - Example of the path (which follows the increment of the window length) resulting from iterative evaluation of the best performance (mean over subjects) for the EVD algorithm extracting the RVMT component. Each point is associated to the similarity result and other parameters obtained in the growing space spanning a number of ICs and window lengths. Given the trade-off criteria, the optimal point is then chosen and reported in tables 5.2,5.3, 5.4

time was < 35 TRs (200 s) and for which the significant temporal correlation with the reference time course was obtained (p value<0.05). The ICA algorithms that offered the best trade-off between high spatial/temporal correlation and low computation time were evd, jade-opac and amuse.

Following a similar format Tables 5.3 and 5.4 summarize the group performance results for the cases in which spatial and temporal *a priori* information was used in ICA algorithms, respectively. Only 4 of the 14 considered ICA algorithms allowed the evaluation of *a priori* information. The constrained ICA algorithm was the fastest performing algorithm relative to the others, almost by two orders of magnitude. A comparison between tables 5.2 to 5.4 shows the advantages of using prior information with some of the tested algorithms. In particular, for constrained ICA the spatial similarity improves by a factor of more than two with either spatial or temporal *a priori* information at negligible cost in computation time. Also, with the use of *a priori* information the fastest algorithm (constrained ICA, computation time < 0.15s) is about two orders of magnitude faster than those giving comparable spatial similarities without priors.

Algorithm	DMN					RVMT					LVMT					NOISE				
List	SS	TC	CT	MO	WL	SS	TC	CT	MO	WL	SS	TC	CT	MO	WL	SS	TC	CT	MO	WL
Infomax	-	-	-	-	-	-	-	-	-	-	-	-	-	-	-	-	-	-	-	-
Fast ICA	0.41(0.02)	0.83(0.09)	23.07(2.02)	13.50(1.50)	18.50(2.50)	0.73(0.08)	0.95(0.03)	19.64(14.93)	16.00(11.00)	21.50(8.50)	0.49(0.04)	0.87(0.03)	17.46(2.48)	11.00(3.00)	30.00(0.00)	0.35(0.11)	0.75(0.17)	22.16(2.93)	13.00(1.00)	21.00(0.00)
Erica	-	-	-	-	-	-	-	-	-	-	-	-	-	-	-	-	-	-	-	-
Simbec	-	-	-	-	-	-	-	-	-	-	0.31(0.03)	0.47(0.08)	0.09(0.02)	22.50(4.50)	24.00(6.00)	-	-	-	-	-
Evd	0.41(0.01)	0.84(0.03)	0.10(0.05)	13.00(8.00)	33.00(2.00)	0.64(0.07)	0.91(0.02)	0.05(0.01)	6.00(3.00)	27.00(4.00)	0.57(0.00)	0.94(0.00)	0.07(0.01)	6.00(4.00)	34.50(0.50)	0.41(0.17)	0.89(0.05)	0.09(0.05)	12.50(10.50)	27.50(2.50)
Jade Opac	0.37(0.05)	0.77(0.02)	11.45(10.11)	21.00(9.00)	21.00(9.00)	0.69(0.04)	0.92(0.03)	10.55(2.23)	27.50(1.50)	27.50(1.50)	0.43(0.05)	0.75(0.00)	18.17(3.38)	30.00(0.00)	30.00(0.00)	0.30(0.07)	0.79(0.10)	0.90(0.60)	12.00(3.00)	12.00(3.00)
Amuse	0.34(0.02)	0.68(0.02)	0.13(0.02)	33.00(2.00)	33.00(2.00)	0.53(0.06)	0.76(0.01)	0.10(0.03)	28.00(3.00)	28.00(3.00)	0.32(0.00)	0.82(0.05)	0.14(0.00)	34.50(0.50)	34.50(0.50)	0.37(0.15)	0.88(0.04)	0.13(0.02)	32.00(3.00)	32.00(3.00)
SDD ICA	-	-	-	-	-	-	-	-	-	-	-	-	-	-	-	-	-	-	-	-
Semi-blind Infomax	-	-	-	-	-	-	-	-	-	-	-	-	-	-	-	-	-	-	-	-
Constrained ICA (Spatial)	-	-	-	-	-	-	-	-	-	-	-	-	-	-	-	-	-	-	-	-
Radical ICA	-	-	-	-	-	-	-	-	-	-	-	-	-	-	-	-	-	-	-	-
Combi	0.41(0.03)	0.75(0.02)	25.13(1.74)	25.50(2.50)	25.50(2.50)	0.70(0.06)	0.93(0.05)	18.36(0.21)	23.50(1.50)	23.50(1.50)	0.49(0.02)	0.69(0.13)	25.13(1.74)	25.50(2.50)	25.50(2.50)	0.28(0.28)	0.49(0.49)	12.89(12.89)	12.50(12.50)	12.50(12.50)
ICA-EBM	0.40(0.01)	0.89(0.06)	10.92(0.39)	13.50(2.50)	13.50(2.50)	0.66(0.02)	0.93(0.05)	29.23(0.58)	25.50(2.50)	25.50(2.50)	0.48(0.00)	0.77(0.04)	29.37(0.72)	28.00(0.00)	28.00(0.00)	0.36(0.14)	0.79(0.19)	10.64(0.81)	15.50(1.50)	15.50(1.50)
FBSS	-	-	-	-	-	-	-	-	-	-	-	-	-	-	-	-	-	-	-	-

Table 5.2: ICA no *a priori* - Results of best performing runs for all available ICA algorithms for a growing length of time window up to 35 TRs and no *a priori* information considered. For each ICA algorithm the best obtained combination of the values of similarity (Sim) and computational time (CT), temporal correlation (TC), model order (MO) and window length (WL) w.r.t. four reference ICs representing brain activities of interest (Fig. 4), is reported. In the table only the results for which the temporal correlation between extracted time course and reference ICs showed to be significant (p-val <0.05) are reported.

Algorithm	DMN					RVMT					LVMT					NOISE				
List	Sim	TC	CT	MO	WL	Sim	TC	CT	MO	WL	Sim	TC	CT	MO	WL	Sim	TC	CT	MO	WL
Fast ICA	0.35(0.04)	0.85(0.05)	24.29(3.24)	16.50(1.50)	23.50(7.50)	0.68(0.12)	0.95(0.03)	15.67(4.72)	13.00(3.00)	26.00(9.00)	0.49(0.08)	0.85(0.09)	17.02(11.92)	10.50(6.50)	31.50(1.50)	0.29(0.07)	0.74(0.23)	17.75(4.33)	12.00(1.00)	20.00(9.00)
Constrained ICA (Spatial)	0.41(0.10)	0.65(0.12)	0.13(0.02)	31.00(4.00)	31.00(4.00)	0.76(0.05)	0.75(0.00)	0.13(0.02)	31.00(4.00)	31.00(4.00)	0.71(0.01)	0.49(0.05)	0.15(0.00)	35.00(0.00)	35.00(0.00)	0.06(0.06)	0.23(0.23)	0.08(0.08)	17.50(17.50)	17.50(17.50)
ICA-EBM	0.32(0.01)	0.84(0.13)	10.92(0.39)	13.50(2.50)	13.50(2.50)	0.62(0.01)	0.98(0.00)	13.46(4.70)	13.50(1.50)	13.50(1.50)	0.27(0.03)	0.77(0.12)	21.24(13.73)	14.00(4.00)	14.00(4.00)	0.34(0.12)	0.84(0.11)	13.46(4.70)	13.50(1.50)	13.50(1.50)
FBSS	-	-	-	-	-	-	-	-	-	-	-	-	-	-	-	-	-	-	-	-

Table 5.3: ICA spatial *a priori* - Results presented as in 5.2, but considering only the algorithms which permit the inclusion of spatial a priori knowledge. Results for which even the temporal correlation between extracted time course and reference ICs showed to be significant (p-val <0.05) are reported.

Algorithm	DMN					RVMT					LVMT					NOISE				
List	Sim	TC	CT	MO	WL	Sim	TC	CT	MO	WL	Sim	TC	CT	MO	WL	Sim	TC	CT	MO	WL
Fast ICA	0.39(0.01)	0.88(0.01)	25.27(8.33)	17.00(1.00)	24.50(8.50)	0.68(0.12)	0.95(0.02)	19.71(0.68)	14.50(1.50)	25.00(10.00)	0.48(0.04)	0.84(0.02)	21.50(1.11)	14.00(2.00)	32.00(3.00)	0.34(0.11)	0.76(0.16)	25.46(6.41)	15.00(1.00)	20.00(1.00)
Constrained ICA (Spatial)	0.41(0.10)	0.65(0.12)	0.13(0.02)	31.00(4.00)	31.00(4.00)	0.76(0.05)	0.75(0.00)	0.13(0.02)	31.00(4.00)	31.00(4.00)	0.71(0.01)	0.49(0.05)	0.15(0.00)	35.00(0.00)	35.00(0.00)	0.06(0.06)	0.23(0.23)	0.08(0.08)	17.50(17.50)	17.50(17.50)
ICA-EBM	0.37(0.01)	0.69(0.13)	18.13(8.29)	16.50(2.50)	16.50(2.50)	0.62(0.05)	0.98(0.00)	10.92(0.39)	13.50(2.50)	13.50(2.50)	-	-	-	-	-	0.38(0.14)	0.92(0.06)	13.81(4.35)	13.00(1.00)	13.00(1.00)
FBSS	-	-	-	-	-	-	-	-	-	-	-	-	-	-	-	-	-	-	-	-

Table 5.4: ICA temporal *a priori* - Results presented as in 5.2, but considering only the algorithms which permit the inclusion of temporal a priori knowledge. Results for which even the temporal correlation between extracted time course and reference ICs showed to be significant (p-val <0.05) are reported.

5.4 Discussion

The aim of the present study was to evaluate the performance of ICA algorithms in ill-posed conditions, i.e. with a small amount of data availability and constraints on computational time. The issue here was to understand if it is possible to adapt an ICA algorithm to a none-ideal environment, as presented in (Esposito et al., 2003). Moreover the analysis has been extended to investigate which ICA algorithm is more suitable to this kind of conditions from the perspectives of monitoring a brain activity of interest.

Testing ICA algorithms in ill-posed conditions must deal with several intrinsic ambiguities and problems, both theoretical and practical, which must be taken into account. In particular, one issue is the comparison of algorithms using different model orders and information. Our goal was to explore the performance in terms of ability to reach the spatial and temporal network characteristics that can be derived from the full dataset in a standard offline analysis. Thus, we assumed as reference the optimal results obtained via group ICA with all time-points available, a model order of 20 and using the infomax algorithm, considering stochastic differences not critical. Another intrinsic issue is due to the fact that the differences in results between off-line and ill-posed conditions can be related not only to computation, but also to the extraction of dynamic behaviour with respect to the stationary one typically extracted by off-line ICA.

One issue that deserves special consideration in these simulations is that of circularity. The use of a validating reference template obtained from the same data used in the simulations does not introduce circularity issues since we are in principle just checking that the same information can be extracted in different ways, with only differences due to noise.

A practical issue to consider is that the high dimensionality of the space of parameters results in a high computational load to run the simulations spanning the entire multidimensional parameter space. The best performance can be evaluated in a trade-off perspective, since different combination of parameters can give similar results. The consequence of this is that the optimality of performance is heavily connected to the practical application and conditions in which the ICA algorithm will be adopted.

Relying on these elements, we perform a direct comparison of different algorithms, defining a cluster of algorithms on the basis of the manipulability of the parameters

that they offer (Tab. 5.1). In fact the tested ICA algorithms can be divided into three groups: those which accept setting of model order and *a priori* knowledge (i.e. infomax, fastICA, semi-blind infomax), those which do not accept neither setting of model order nor *a priori* knowledge (i.e. jade-opac, amuse, radical ICA, combi), and those which accept only one of the two (i.e. erica, simbec, evd, constrained ICA, ICA-ebm, FBSS). These constraints were intrinsic to the algorithms as in their public distributions. It was beyond the scope of this work to try to change any of the algorithms to eventually make them more flexible. The more flexible algorithms (i.e. those accepting full manipulability of parameters) will not necessarily be better, since the most rigid could be the most adaptable for specific circumstances. Putting everything in a real-time fMRI experiment perspective, it is possible to distinguish the algorithms on the basis of the tasks and conditions they must face. Those algorithms which do not accept any *a priori* knowledge could work very well to define the target networks from the functional localizer step that usually precedes a real-time fMRI acquisition, a step in which *a priori* knowledge may not be necessary or even available. For this use it is possible to permit a higher computational load, since usually the localizer part of an experiment can have more time allocated to it. The algorithms that tended to be more suitable for this use are evd and amuse, which result in particularly fast computation, with evd performing slightly better. The jade-opac and fastICA algorithms also performed well but at the cost of a higher computational time (Tab. 5.2). The results show that the use of *a priori* knowledge can drastically improve computation time and spatial similarity to a target IC. This suggests that use of priors may be crucial in the dynamic analysis part of the real-time fMRI experiment, where any information from the localizer can be exploited to speed up the process and increase accuracy. From this point of view the flexibility of the ICA algorithm is essential. Thus among the algorithms which accept *a priori* knowledge, constrained ICA provides the most optimal solution, followed by fastICA (Tables 5.3 and 5.4).

For completeness, it is important to analyse the values of the two parameters growing window length and model order for the previously reported best performing algorithms. In an on-line perspective these values are related to the time needed to elapse before obtaining the first real-time result or step updating. This means that the longer the window and the higher the model order, the more time will pass before the availability of results. If this can be not critical for a functional localizer step, it is relevant

to the on-line computation, since the scale of the resolution in monitoring the brain dynamics will be directly associated to that. This means that different algorithms can shown to be more or less adapt to be directly exported to a real-time set-up.

Another observation is related to the type of brain activity monitored (i.e. if it represents a resting state brain activity, a task related activity or physiological noise). Monitoring ICs with different origins conveys different information. Variability in the capability of ICA algorithms to correctly extract target ICs can be directly justified by the fact that the less variance of data is explained by the IC, the more difficult is to extract it by decreasing the amount of data available. For this reason ICs whose rank is low in a canonical ICA decomposition are critical to identify in the ill-posed conditions. Nonetheless, as the simulations show they can still be identified.

The periodicity of the ICs of interest affects the choice of optimal parameters. From simulations it can be seen that a significant performance may be reached even reducing the data to a single period of the task in the ICs of interest. The DMN deserves particular considerations due to the low frequency nature of its signal sources. Its identification, despite being easily done by data driven algorithm, is dramatically harder in ill-posed conditions given that its periodicity is significatively longer, thus it results difficult to observe enough of its dynamic given the real-time compatible vincula on time window length. Given these new dimensions (type of brain activity and periodicity) it is possible to see that different algorithms have different effectiveness in adequately identify brain activity coming from different kinds of sources. It can be seen that the same algorithm can outperform all the others in detecting task related activity, while suffering in dealing with non-structured noise or, viceversa, as for example it happens in the case of evd and jade-opac, or evd and combi with no *a priori* knowledge. The same reasoning holds for the use of *a priori* knowledge. Even if in this case not all algorithms permit the introduction of *a priori* knowledge in performing the ICA decomposition, for those which accept this input the performance varies considering different target sources. Indeed fastICA and constrained ICA alternate best performance, with constrained ICA performing slightly better overall.

Additional ambiguity comes from the stochastic nature of most ICA algorithms, resulting in different runs of ICA delivering slightly different results. This is due to the search procedure of final results optimization, which results in the algorithm being trapped in a local minima. Another observation can be related to the computational

time of ICA decomposition: in general it grows linearly with the increase of the window length, and this can be easily justified by the fact that the more data are to be processed the more time it takes to do that. But as the data become more descriptive of the source to be extracted, the algorithm is able to extract it easier, thus reducing the computational time needed, independently by the data length.

One limitation of this study is that the adopted implementations of ICA algorithms are not directly optimized for ill-posed conditions. This opens the doors to further development oriented towards their methodological and algorithmic optimization, which would make them more efficient and flexible. Another element to be taken into account is the relatively small number of subjects adopted in the simulations. This constraint was driven by the necessity of having a dataset whose behaviour was well known in the ICA domain and which could confirm the stability and validity of obtained results. Nonetheless, this work demonstrates a methodology for evaluating different ICA implementations for the purpose of finding the ICA algorithms and analysis parameters for the optimal detection of a target brain network under ill-posed conditions. Further experiments are needed to evaluate the performance of ICA implementations on larger datasets and also other networks.

The results of this study can be used to evaluate ICA implementations for the dynamic analysis of fMRI data. In particular, in a potential real-time fMRI perspective, the best performing ICA algorithm without the use of *a priori* knowledge can be adopted to analyse the functional localizer data in a data-driven way. In this approach the target ICs to be then followed dynamically in the real-time experiment are defined without considering spatial or temporal constraints. The sources defined by the functional localizer can then be used in different algorithms that include *a priori* spatial, temporal or spatio-temporal knowledge for the dynamic monitoring of target ICs in a real time fMRI experiment, such as for neurofeedback.

5.5 Conclusions

In this chapter we presented an extensive comparison of ICA algorithms under the constraints to have a fast decomposition with a small amount of data available (ill-posed condition). The aim of ICA is to exploit the multivariate nature of data driven

methods to perform a whole brain analysis. Here we have shown that ICA can satisfactory work in ill-posed conditions with results which are similar and thus acceptable with respect to the off-line implementation. In our comparison we found that several ICA algorithms (evd, jade-opac, fastICA, constrained ICA) can be adopted in ill-posed conditions and thus can be exploited for dynamic analysis of fMRI data. The best performing algorithms (evd, constrained ICA) show to be also robust against errors in parameters, and are fast in terms of computational time. This opens the door to their exploitation in applications such as real-time fMRI, both as functional localizer and on-line dynamic analysis. Adoption of these methods would be useful for experimental designs such those known as neurofeedback experiments, although further work is needed to implement a fully real-time ICA method for fMRI data analysis.

6

Experiment 3: Evaluating novel methods for real-time fMRI by use of *a priori* conditions

6.1 Introduction

In *Chapter 5* the performance of 14 different ICA algorithms considering also as variables the model order and different types of *a priori* knowledge (spatial/temporal) (Soldati et al., 2012) has been evaluated. This work showed that ICA algorithms such as EVD, amuse, jadeopac, FastICA are suitable when implemented in the identification phase via a functional localizer since they perform well even without extensive use of *a priori* knowledge. It is interesting to note that FastICA algorithm represents a good trade-off and its performance is valid in both functional localizer and dynamic monitoring phases. Other algorithms like constrained ICA performed worse without *a priori* knowledge and may thus be more suited for the dynamic monitoring phase due to their ability to incorporate *a priori* knowledge. Such *a priori* knowledge may help guiding the algorithm to detect a specific target IC with higher priority over the other ICs present in the data. However, there are several types of prior information that are available including spatial domain, the temporal domain, or both, and any of these could be used in different ways (as constant references from a localizer or derived dynamically). It is however not clear how these various ways of using priors may affect the performance of the results both in terms of computation time and correlation to

a reference optimal ICA. Moreover, the ICA algorithm (FastICA) is stochastic, which means that multiple repetitions of the analysis on the same dataset can give slightly different results, both in the spatial and temporal domains. This problem has been extensively discussed in literature, where one of the main proposed solution has been a method based on multiple ICA runs and clusterization of the obtained components, with the aim of reducing the issue of stochastic variability (Himberg et al., 2004). Such instabilities can be characterized by the standard deviation of the derived (STD) results (spatial and/or temporal) when the analysis is repeated multiple times on the same dataset. The STD can be considered as a stability performance parameter of the algorithm, lower STD algorithms corresponding to more stable ones. This parameter may be particularly relevant if different ICA-based algorithms are to be considered and compared for real-time fMRI, where the analysis is repeated dynamically during data acquisition.

In this chapter we exploit results from the previous chapter and extend them by proposing and evaluating novel ICA-based algorithms that use different types of *a priori* knowledge for the dynamic monitoring of ongoing fMRI activity. The *a priori* information considered is either temporal, spatial, or both spatial and temporal. In addition, the *a priori* information is considered both in its static version when derived from the functional localizer, as well as dynamic when estimated recursively as the sliding-window progresses over the time course throughout the run. The different analysis methods are tested by simulating a real-time fMRI experiment using an existing and public dataset. In this sense there is no feedback signal. The performance measures used to compare the various algorithms are based on the spatial and/or temporal correlation between the independent component (IC) estimated dynamically and the target IC derived from the localizer, computation time and intrinsic stochastic variability of the algorithms.

6.2 Materials and Methods

We refer the reader to the Appendix for details on the acquisition paradigm for the fMRI dataset adopted in the analysis performed in both Chapter 4 and 5.

6.2.1 Analysis Framework

The proposed framework for performing rt-fMRI exploiting a multi-variate and data-driven approach is based on the structure schematically presented in Fig. 6.1. The general structure and workflow can be outlined as follows:

1. The MR data acquired by the scanner is stored during acquisition and made available to the data analysis system as soon as the images are reconstructed.

2. At the beginning of the experiment a short period (typically about 5 min. or less) is devoted to acquire data from a FL. In the proposed framework the FL data is analyzed using a blind (unconstrained) ICA algorithm to preserve the multivariate data-driven advantages. Others have used univariate methods at this stage (Esposito et al., 2003).

3. An IC of interest is selected from the FL analysis, this IC becomes the data-informed multivariate ROI whose activity is to be monitored dynamically.

4. The IC of interest, along with possible *a priori* information, can be incorporated in the rt-ICA data analysis algorithm. The ICA algorithm uses a sliding window approach and a blind source extraction (BSE) perspective to deliver results at each TR while updating the best match to the target component. This monitored component or other *a priori* knowledge is then provided recursively to the algorithm, which extracts the actual version of the monitored IC updated by the actual values of data.

5. The monitored IC can be used as in classical rt-fMRI paradigms for visualization, neurofeedback or brain computer interfaces. The component selected in real-time is the one that has a spatial map which maximally correlates with the reference spatial map component identified during the Functional Localizer (FL) step. The spatial FL component corresponds in turn to the FL component whose temporal correlation with the timing of the paradigm is highest.

As previously discussed, an effective application of the monitoring phase requires one to explore the effectiveness of different methods for performing the on-line analysis. The methods studied in this work are static approaches using back-projection and dynamic methods based on iteratively performed ICA. In particular, for the dynamic

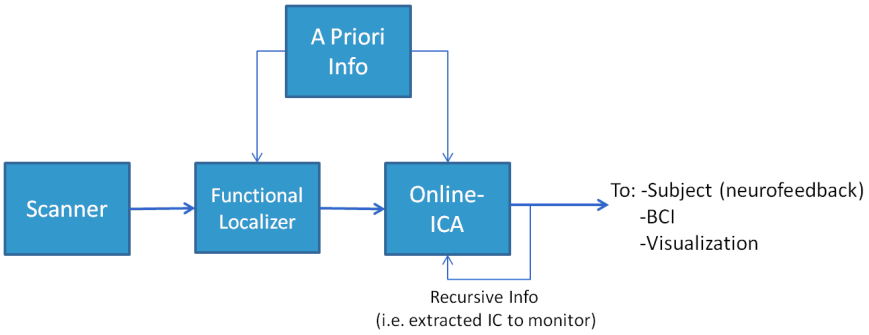

Figure 6.1: Experiment 3- Design Framework - In this structure it is possible to identify two main phases (or steps). The first step is to identify what one should monitor, i.e. performing a Functional Localization. This can be done with or without incorporating some kind of *a priori* knowledge. The second step is to monitor the phenomenon we identified in the previous step using a suitable on-line analysis method.

methods, FastICA and constrained ICA are updated for a sliding-window real-time fMRI implementation. The size of the sliding window was chosen based on previous work that systematically evaluated the performance of multiple ICA algorithms as function of window length amongst other variables (Soldati et al., 2012). This study showed that the sliding window length that gave the optimal trade-off between computational speed and spatial/temporal correlation with the results from the whole time course was approximately equal to the period of the behavioural task to be monitored. In our experiment this can be approximated to around 30 seconds, i.e. 15 TRs. It is worth noting that the size of this window, as pointed out in the discussion, is strongly related to the period of the behaviour to be monitored.

6.2.2 Accuracy Estimation and Template Creation

To estimate the accuracy of one technique in correctly describing a monitored IC at one arbitrary time point we compare the temporal correlation and spatial overlap of the dynamically reconstructed IC with the same IC obtained using the whole time course. In order to do that, it is necessary to create the templates of ICs which will be taken into account as reference data to evaluate the quality of rt techniques. These templates represent the principal characteristics of the ICs to be monitored during the simulation. To this end an ICA analysis is performed on the single subject level by considering all time points (i.e. 220 TR), but using FastICA with the same model

order to be used in the on-line implementation (i.e. 5). Three different target ICs were selected to simulate their dynamic monitoring see Figure 6.2: two task-related components (RVMT and LVMT) and the task-induced default mode network (DMN).

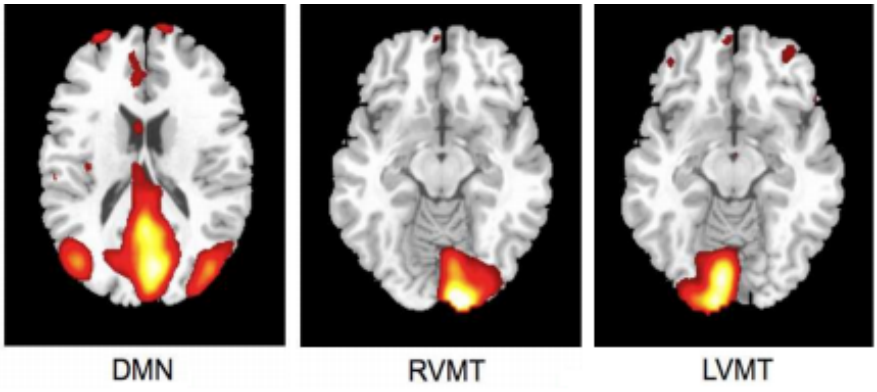

Figure 6.2: Experiment 3- Monitored ICs. - An illustrative example of the monitored ICs is reported. Spatial maps of ICs considered in the simulation are obtained from Group ICA 20 ICs. For ease of visualization only the relevant slices are reported here. First column depicts Default Mode Network (DMN). Second and third columns depict the two task relatedICs , Right Visuo-Motor Task (RVMT) and Left Visuo-Motor Task (LVMT).

6.2.3 Functional Localizer

In a rt-fMRI experiment the functional localizer can be used to identify the IC to be later dynamically monitored. For the analysis of the FL we consider the use of full whole brain ICA to maintain a multivariate data-driven method. Previous simulations suggest that the ICA analysis of the FL data is most accurate when using algorithms such as evd, jadeopac or FastICA (Soldati et al., 2012). We chose the FastICA algorithm with a model order of 5, the same algorithm used in the template creation. In our simulation the FL data portion was taken from the first 60 TRs of each subject's time series. With the application of FastICA as FL an unmixing matrix W is estimated of dimension 5 by number of time points. Each row of the matrix represents a time course of an hidden source, and the associated row of the X derived matrix represents the corresponding spatial map.

6.2.4 On-line Techniques

In this section we present the main novel component of the developed work, that is the methods implemented to perform the on-line monitoring of the sources. Given that the target is to properly exploit the *a priori* knowledge, different approaches to combine this knowledge and the ICA algorithms have been developed. In a comprehensive perspective all the possible combinations have been explored. Starting from the concept of sliding-window ICA as it has been presented in Esposito et al., 2003, more sophisticated methods have been implemented. The target has been to obtain an actual temporal value of the activation of interest and/or an actual spatial map of this component. Two main criteria were the guidelines in these implementations, that is the dynamic of the data and the type of *a priori* knowledge. The dynamic criterion means how much novel information is exploited and weighted into the on-line method, while the type of information exploited denote the nature of the *a priori* knowledge, i.e. temporal, spatial or both. The implementation exploited state of the art ICA algorithms (FastICA, Constrained ICA) with the target of making the implementation easy to reply and distribute.

The following subsections present the details of the different on-line monitoring techniques proposed.

6.2.5 Static Method: Back-projection [BP]

This method is based on the assumption that the ICA performed as FL is able to create a space described by the directions of the extracted ICs that is fairly representative of the brain state during the performance of the task of interest. This means that the spatial map (SM) of an IC of interest obtained by the FL can be kept fix. Under this assumption, it should then be possible to simply back project each newly acquired volume of data into this space (i.e. SM of the IC of interest) to be able to quantify the contribution in the new data of the brain activity of interest, i.e. the time course of the IC.

This means that from FL exploiting FastICA it is possible to estimate an unmixing matrix $W = A^{-1}$ and thus the associated SM of the sources $X_{nIC,v}$ with nIC equal to the number of extracted components (5 in this case), and v equal to the number of voxels. The SM of the desired component is then chosen as the source whose associated

time course is the most correlated to the task of the FL, that is we have a selected IC *sel* such as $X_{nIC=sel,v}$. At this point, for each newly acquired volume $Y_{i^{th}}$ of dimension one by number of voxels we can compute:

$$a_{i^{th}} = Y_{i^{th}} X'_{nIC=sel,v} \tag{6.1}$$

where $a_{i^{th}}$ is the actual single time value of the IC of interest). It is worth noting that this can be straightforwardly extended to cases in which multiple components are monitored simultaneously via extending the dimension of the Y and X matrices.

6.2.6 Dynamic Method: Recursive Temporally Constrained [RTC]

This algorithm is a direct extension of that used by Esposito et al. (Esposito et al., 2003). The main differences are that here it is applied to the whole brain and that the computation of *a priori* temporal knowledge is not model-driven, but it is rather data-driven and obtained with an approach based on the previously presented back-projection method. The actual difference with the back-projection technique, in which the SM is static, is that we obtain an actual updated SM via ICA computation, which is based on the temporal *a priori* information of the IC of interest. In this approach we use the FastICA algorithm with model order 5 and time window length 15 TR, and the *a priori* temporal constraint is given in terms of an initialization of the mixing matrix A.

In practice a sliding window of dimension nTP is updated for each newly acquired volume n leading to a matrix $Y_{[n-nTP,n+nTP],v}$ of dimension nTP by number of voxels. This matrix and the SM obtained in the FL step (i.e. $X_{nIC=sel,v}$) are used to extract a time course in a data driven way in the same fashion as for back-projection algorithm, resulting in a time course a_n of dimension nTP by one. With the actual data matrix $Y_{[n-nTP,n+nTP],v}$ and the time course a_n it is then possible to apply FastICA to extract the actual SM of the component of interest. This is done by initializing the first entry of the W matrix with the inverse of a_n, given that $W = A'$, in the routine presented in the ICA mathematical preliminaries section. The result is the actual SM IC (i.e. $Xnew$) present in the data whose behaviour is closest to the reference time course. In other words the extracted IC is constrained to be as close as possible to the reference one at the initial step, permitting a much more dynamic computation of the IC and

thus update of the monitoring. In this approach the SM is dynamically updated each time a new volume is acquired.

6.2.7 Dynamic Method: Recursive Spatially Constrained [RSC]

As in the previous method, also in this dynamic method, the on-line monitoring requires a continuous update of the ICA decomposition matrix. This matrix is obtained from the joint contribution of information derived from the actual newly acquired data and the *a priori* information available. In particular, the method based on spatial constrains foresees the use of a spatially constrained ICA algorithm (constrained ICA (Lin et al., 2010)). In this approach, the knowledge of an *a priori* spatial map of the IC of interest permits to constrain the computation of the ICA algorithm. In details, the extracted IC, although being based on newly acquired data, is forced to be spatially as close as possible to the spatial *a priori* given map (i.e. to the SM obtained during FL).

The associated time value will be given by an approach similar to the back-projection method but depending on the dynamically updated SM, i.e., given the new SM (i.e. $Xnew$), by computing $a_{i^{th}} = Y_{i^{th}} X'_{new}$.

6.2.8 Dynamic Method: Recursive Spatio-Temporal Method [RSTC]

This algorithm implements the possibility of obtaining actual values of both time course and spatial map with two concatenated steps. This is obtained by combining the previous described methods to obtain a fully updating on-line method based on the following steps:

1. Back-project the actual data on the SM of FL, obtaining the actual value of time course in the FL space $a_{FL} = Y_{i^{th}} X'_{nIC=sel,v}$ (note that in the BP algorithm we assume little or no difference between the template space and the actual subject space).

2. Apply the temporally constrained algorithm (i.e. initialize the W matrix exploiting the a_{FL}) to obtain the SM (i.e. X_{sub}) in the actual subject space (note that this is different from the FL space).

3. Apply the spatially constrained ICA with the SM in the actual subject space to obtain the actual time course value in the subject space, that is $a_{sub} = Y_{i^{th}} X'_{sub}$.

6.2.9 Variability effects from the stochastic nature of ICA

ICA methods (with some exceptions like the jade algorithm) are typically non deterministic since there is a stochastic component in the analysis. This introduces a variability each time the algorithm is run, which in turn can affect the computation time and the performance of the dynamic monitoring of a target IC. Such variability effects were investigated by repeating the analysis 10 times for each subject on the same data, and then computing the standard deviation across repeated trials for the mean correlation between dynamic and template spatial maps and temporal time course.

6.3 Results

Using publicly available fMRI data from a previous experiment (Calhoun et al., 2001) we simulated a real-time acquisition in a sliding window approach to evaluate the performance of four implementations of ICA with different uses of *a priori* information: i) back-projection of constant spatial information derived from a functional localizer (BP), ii) dynamic use of temporal (RTC), iii) spatial (RSC) or iv) spatio-temporal ICA constrained data (RSTC).

Given the stochastic nature of the ICA algorithms used, the variability of the spatial and temporal results was evaluated for each subject on each of the target networks (Default Mode Network (DMN), Right Visual Motor and Left Visual Motor Task related components (RVMT and LVMT respectively)) and for each of the four ICA implementations. The results showed in Figure 6.3 point out that stochastic effects can introduce variability in the performance of the IC order ranking accuracy up to 10 %, sometimes producing large fluctuations. This behaviour suggests that none of the four ICA implementations gives consistently the lowest sensitivity to fluctuations due to stochastic effects, although the BP method tends to be the lowest in 15 out of 18 cases.

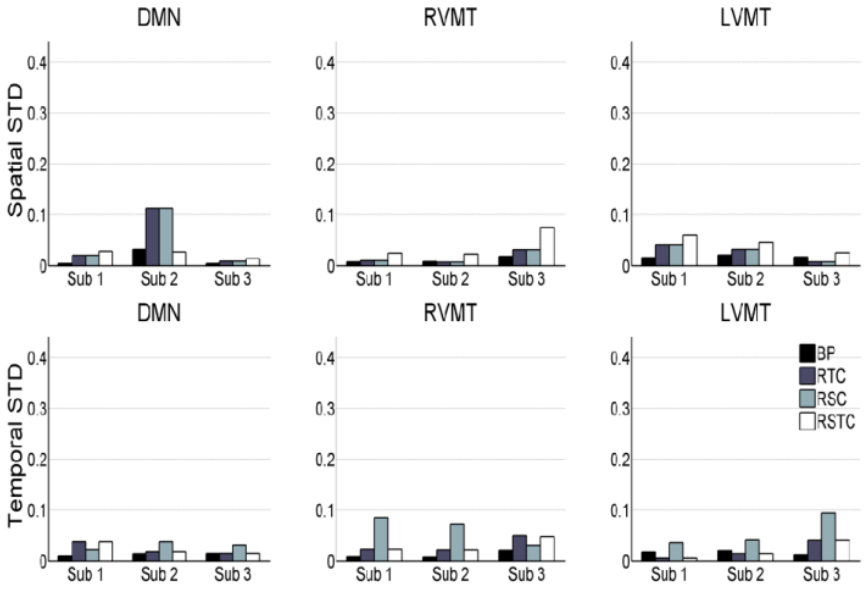

Figure 6.3: Experiment 3- Variability of dynamic tracking performance results due to the stochastic nature of ICA. - Performance is here represented by two metrics: spatial or temporal correlation between the template and the dynamically tracked IC, averaged along the time course. The calculations were repeated 10 times for each subject, for each of the three networks evaluated (default mode or DMN, right visual motor or RVMT and left visual motor or LVMT) and for each ICA implementation (back-projection or BP, temporally constrained or TC, spatially constrained or SC, spatio-temporal constrained or STC). The variability of the dynamic tracking performance results is expressed as the standard deviation across trials, per subject, brain network and ICA implementation.

Proceeding with further analysis it is possible to focus on the evaluation of stability of results across subjects and across different monitored ICs, as presented in Figure 6.4. This figure reports the standard deviation across subjects of the mean (across trials, for each subjetct) spatial and temporal correlation for the monitored ICs.

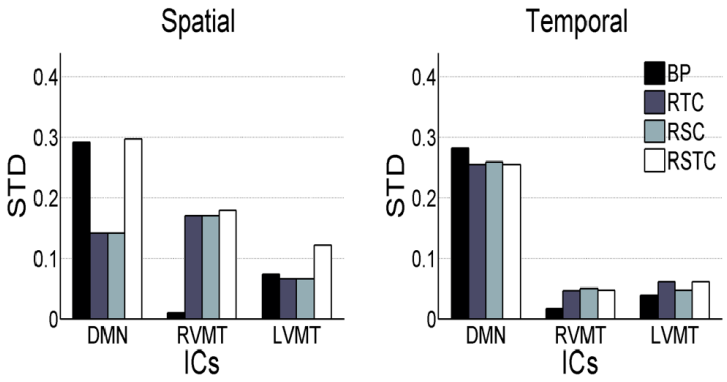

Figure 6.4: Experiment 3- Variability of dynamic tracking performance results due to subjects. - Similar to Figure 6.3, but here mean results across trials are used to compute variability across subjects, expressed as standard deviation. The subject variability is shown for each of the three networks evaluated (default mode or DMN, right visual motor or RVMT and left visual motor or LVMT) and for each of the four ICA implementations (back-projection or BP, temporally constrained or TC, spatially constrained or SC, spatio-temporal constrained or STC).

Finally the performance evaluation numbers are reported in Figure 6.5 and Table 6.1, in which one can seen the spatial and temporal correlation between the reconstructed time courses and spatial maps of the monitored ICs and the reference templates of those ICs.

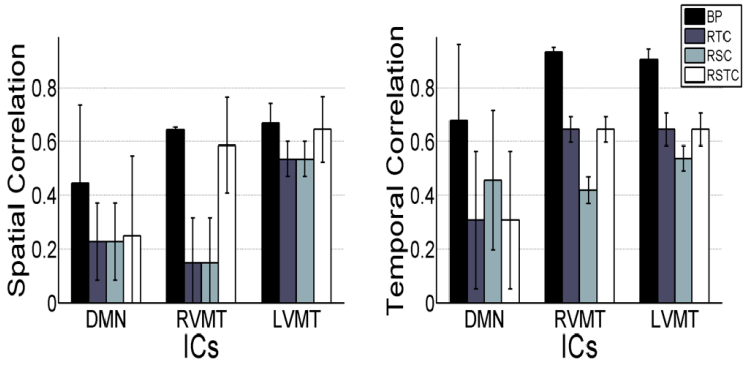

Figure 6.5: Experiment 3- Overall dynamic tracking performance in reconstructing ICs. - The mean and standard deviation performance results are shown across subjects and trials in terms of both spatial and temporal correlation with the template ICs. The results are shown for each of the three networks evaluated (default mode or DMN, right visual motor or RVMT and left visual motor or LVMT) and for each of the four ICA implementations (back-projection or BP, temporally constrained or RTC, spatially constrained or RSC, and spatio-temporal constrained or RSTC).

The table reports the performances in terms of computational time necessary to update the the actual value of time course or spatial maps for each new available data volume. This represents another critical issue of a real-time analysis.

Online Method	CT[s]		
	DMN	RVMT	LVMT
Backprojection	0.0056 (0.0002)	0.0054 (0.0004)	0.0054 (0.0007)
Temporally Constrained	2.3 (0.4)	2.1 (0.1)	2.0 (0.3)
Spatially Constrained	0.119 (0.003)	0.1167 (0.0002)	0.1169 (0.0003)
Spatio-Temporally Constrained	0.123 (0.003)	0.1207 (0.0002)	0.1208 (0.0002)

Table 6.1: Proposed Methods Performances - This table summarizes the performance results in terms of computational time (CT) from all the investigated rt-ICA techniques relative to the different monitored ICs. Mean values of updating CT are reported for simulations on three subjects and ten trials per subject. Standard deviations associated to mean values across subjects and trials are shown in parenthesis. The selected ICs to monitor were default mode network (DMN), right visuo-motor task (RVMT) and left visuo-motor task (LVMT).

The results show that the back-projection method offers the highest performance both in terms of time course reconstruction (correlation value to the template time course was significant and quite high, around 0.9), and speed (computation of update value was far below the TR). This method is very fast and effective as far as the monitored IC has a strong and well defined behaviour and/or it is well extracted in the FL, since it relies on an accurate description of the spatial behaviour. The fluctuations reported in the figures represent error fluctuations in the FL phase which directly reflect in the back-projection method. The dynamic methods offer comparable performances at cost of higher computational time (CT) (around 2s for RTC). In particular the spatio-temporal method performs comparably in terms of CT to back-projection, offering more variable performances in terms of reconstruction of spatial maps and time courses.

6.4 Discussion

In the present work we presented and evaluated different methods to combine ICA-based algorithms for real-time fMRI. The motivation for this work was to investigate how the advantages of such multivariate data-driven methods can be adapted to real-time fMRI

applications, extending previous work (Esposito et al., 2003). One goal of this work was to simulate a realistic scenario fully based on ICA consisting of two essential steps. The first step is dedicated to identifying brain networks of interest from the ICA of a functional localizer. The second step consisted of dynamically monitoring a target IC (derived from the first step) with the use of different types of *a priori* knowledge in the computations. The *a priori* information considered ranged from static to dynamic, where spatial maps and time courses can be updated separately or together to give more weight to the dynamic monitoring of data within a pre-established time-window in the fMRI time course. The incorporation of *a priori* information is motivated to address the challenge of identifying and keeping track of a specific IC of interest, despite all the other ICs that may be present in the data. This work therefore focuses on evaluating different ways of using prior information about the target IC to monitor such that during the dynamic monitoring phase the target IC can be effectively detected with higher priority relatively to other possible ICs.

The ICA-based techniques presented for the on-line monitoring are characterized by different advantages and disadvantages. Overall findings confirm two general expected features: i) the dynamic monitoring performance is directly related to the strength of activation of the target IC identified in the functional localizer, stressing the importance of this first step, and ii) as algorithms become more adaptive in the use of spatial and/or temporal priors in the dynamic monitoring, they introduce less stability in the performance results compared to off-line results. This reflects the intrinsic differences between static off-line analysis and dynamic one.

The back-projection technique has the positive features of being stable in terms of lowest fluctuation across trial and subjects, very fast relative to the TR of fMRI data acquisition (since it just involves a matrix multiplication), conceptually simple and being able to monitor more than one IC of interest. The main potential disadvantage of the back-projection method is related to its non adaptivity, since it assumes that the target IC of interest is always present with the same properties, i.e. a fixed spatial map is considered.

The temporally constrained ICA is more adaptive to data with respect to back-projection. Even if similar to what presented by Esposito et al. (Esposito et al., 2003), this method offers different characteristics. The main one is that the reference time course used as constraint is not obtained using a hemodynamic model, but it

is extracted from the data in a multivariate data-driven way by the FL. Moreover in this method the reference time course is updated in a similar way to back-projection, while the crucial difference is that the spatial map updates iteratively each time new data become available. A characteristic of the temporally constrained ICA is that the dynamic spatial map generated is derived from the time course used to initialize the ICA algorithm. This time course, being derived from the back-projection of actual data on a static space (i.e. keeping the spatial map of the IC of interest fixed), is strictly related to the quality of the FL. For this reason the time course reconstructed is in the template space (i.e. FL space), while the spatial map is in the subject space, being obtained by exploiting reconstructed time course as *a priori* knowledge during the application of the ICA algorithm. A limitation of the temporally constrained algorithm is that its mean computation time is more than one order of magnitude higher relative to all the other methods tested. This is due to the fact that the FastICA algorithm adopted in it, while performing generally lower than a TR, sometimes (around 2-3 % of the times) gets stuck in a local minimum thus increasing the time to perform the decomposition (in some cases from 1.5 up to 8 seconds). A possible solution to this would be to skip the updating of the information for those volumes which exceed a pre-determined temporal limit to update.

The spatially constrained ICA assumes a fixed spatial map of the IC of interest. This approach suffers from the small amount of data available for the decomposition. The main advantages include low computational time and low variability of the results, qualities that make it a good candidate for the use in real-time experiments.

The combined implementation of spatial and temporal constrained ICA offers potential of better describing the actual dynamic behaviour of data, thus focusing on data characteristics which are strongly transient and for this reason probably not modelled in the off-line static analysis, which privileges extraction of static periodic or quasi-periodic behaviours. This method enables us to obtain valuable results both in terms of accuracy and computational time. Its main disadvantage is that it is less able to characterize static aspects of the data.

A further consideration is needed related to the variability of monitoring performance. Three kinds of variability were investigated in the simulations. The first one is due to the stochastic nature of principal ICA algorithms, which causes different results

to be obtained in different runs of the algorithm on the same data. Multiple repetitions of the analysis showed that this variability can affect computation time, but the obtained performance has a stability better than 10 %. The second kind of variability identified is subject specific which causes about 20 % of the variability. The third source of variability in the dynamic performance monitoring relates to the specific target IC within a subject. Across different monitored ICs within the same subject, the results of Table 6.1 and Figure 6.2 confirm that the difference in behaviour of different subjects is consistent across ICs. Indeed all the subjects improved performance monitoring task related RVMT and LVMT (Figure 6.1) with respect to Resting State Network (RSN) related Default Mode Network (DMN) (Figure 6.2) thus proving that difference in the nature of monitored IC is the strongest source of variability (up to 30%) for these kind of presented methods. This may be due to the fact that different activations have particular statistical distribution properties, being more or less suitable to be extracted by ICA algorithms. In addition, a reason of the difficulty in extracting spatial characterisation of the DMN is its low frequency relative to the the sliding time window length, thus making it difficult for the algorithm to correctly follow it.

This work has some limitations. One limitation is related to the definition of dynamic monitoring performance, which depends on temporal or spatial correlations with a template reference derived from the whole time course. It is not necessarily correct to expect that spatial-temporal characteristics derived from the sliding window along the time course should match the ones derived from the whole time course. For this reason the performance measures are only indicative.

The possibility that the actual dynamic brain activation is correctly identified by these on-line methods opens the door to future definition of techniques and experiments. These experiments could exploit these methods to have a confirmation of transient activation identification independently of the off-line analysis, which represents a general reference for evaluation of results, but may also represent a bias.

Another limitation relates to the simulation nature of the work, which should be further evaluated on a real implementation in which the performance of the different methods can be studied, for example using a neurofeedback setup.

This work proposes and evaluates several strategies for using *a priori* information in ICA-based methods for the monitoring of brain networks in real-time fMRI experiments. The performance of the methods was characterized by both computation speed and

correlation between the spatial-temporal properties of a target independent component derived dynamically and a reference component. The method that gave the highest performance was based on the back-projection of a constant target spatial map derived by the spatial localizer. This method has the limitation that its reference is constant and may not be optimal to follow as it cannot adapt changes in brain. The other tested methods were based on the use of adaptive spatial, temporal or spatial-temporal priors and may have useful applications in studies where there is a need of higher flexibility to monitor variable activation.

6.5 Conclusions

This chapter proposed and evaluated several strategies for using spatial and/or temporal a priori information in ICA-based methods for the monitoring of brain networks in real-time fMRI experiments. The performance of the methods was characterized by both computation speed and correlation between the spatial-temporal properties of a target independent component derived dynamically and a reference component. In our testing conditions of relative low frequency task-induced activations (with a period of 20s) we found that the back-projection method outperformed the other methods giving the highest spatial-temporal correlations to the reference and the fastest computation time. It remains to be further investigated whether the spatial-temporal constrained methods can be better, as in principle expected, in situations where the networks to be monitored have higher frequency fluctuations in space and time.

7

Experiment 4: Evaluating novel methods to fuse multimodal EEG-fMRI data

7.1 Introduction

The recent technical developments and progress in data acquisition systems made available to the scientific community the possibility of jointly and simultaneously acquiring EEG and fMRI data (Purdon et al., 2008). EEG-fMRI is thus becoming a standard acquisition technique, and several groups recently put effort in its implementation and exploitation (Babiloni et al., 2005; Debener et al., 2006). As the technical issues are solved and novel solutions for the improvement of the quality of data are proposed, such as gradient and ballistocardiogram related artefact denoising methods (Assecondi et al., 2009), the attention of the scientific community shifted toward the development of suitable algorithms able to extract the information content present in these two heterogeneous modalities, see *Section 2.3* for details. Several studies showed that the joint exploitation of information derived by EEG and fMRI data permits to overcome the spatial and temporal resolution limits of each separate technique and shed the light over aspects of brain activity which cannot be explained by single modalities (De Martino et al., 2010; Mantini et al., 2007; Martinez-Montes et al., 2004). Nonetheless, the identification of suitable methods to extract and interpret this great amount of available information is a challenging problem, due to the differences in nature and

characteristics of EEG and fMRI data.

Three main approaches have been developed in literature to address these problems. The first two foresee an univariate perspective, that is one modality is assumed do be independent and the other dependent. This is the case where EEG signal is adopted as regressor, convolved with hemodynamic response model and used to explore fMRI data for related activations in voxels (Lemieux et al., 2007). On the other way fMRI data is used as a constraint to solve the inverse problem of source localization in EEG data (Phillips et al., 2002). Both of these methods, although relatively easily interpretable and robust, do not exploit jointly the full information of the two modalities, thus lacking of power from an information theory perspective. A third way is to perform the analysis jointly, via utilization of a model such as in the bayesian framework (Daunizeau et al., 2010) or in kalman filter approach (Deneux and Faugeras, 2009). The exploitation of the model has intrinsic limits due to the difficulty of defining an adequate neurophysiological model for EEG-fMRI data generation and interaction. Due to this reason recently advanced data-driven signal processing algorithms such as Independent Component Analysis (ICA) and Tensorial Decomposition have been explored (Calhoun et al., 2007; Zhao et al., 2012). These data driven methods have shown to be very promising and suitable to address this complex problem. For a recent detailed review see (Sui et al., 2010). In particular Partial Least Square (PLS) (Martinez-Montes et al., 2004) and Joint or Parallel ICA (Calhoun et al., 2007; Eichele et al., 2009) has been adopted with success. PLS is able to find hidden links between the modalities thus obtaining good performances in data decomposition, but resulting in complex and hardly interpretable results due to the use of latent variables. Latent variables are varibles that are not directly observed but are rather inferred (through a mathematical model) from other variables that are observed (directly measured). ICA on the other side showed to be more interpretable but in the current implementations does not exploit jointly the multidimensional information content present in the data, limiting itself to a bidimensional matricization of the datasets. In fMRI this matricization is typically the voxels by time points transformation of the 4D volume of data acquired.

Here we propose a novel procedure to exploit both a tensorial implementation of PLS (Higher Order PLS, or HOPLS) and ICA methods in order to extract jointly the information content that is naturally present in multidimensional data and to find the Independent Components associated to this information. The main idea of this novel

method is to maintain the EEG and fMRI data in their multidimensional domains (respectively tensors of time points, trials, electrodes and tasks for EEG data and voxels, time points, trials and tasks for the fMRI data). In this way, exploiting as common dimension the trial dimension it is possible to apply HOPLS without relying on an haemodynamic filtering model, nor with the necessity of subsampling to make the temporal dimension compatibles between the heterogeneous data. The application of HOPLS will thus extract latent variable and associated factors jointly for EEG and fMRI data, thus partitioning and intrinsically linking the information across factors (i.e. the associated components in the various dimensions of fMRI and EEG data) and modalities. Each of these factors can be subsequently separately analysed by any desired BSS method, like FastICA.

The goal is to verify that HOPLS is able to meaningfully extract linked components in EEG and fMRI data domains. In order to have a metric of reliability on claim about how much meaningful are the identified components a classification approach is implemented and exploited as described in section 7.2.6. The method has been tested on a simultaneously acquired EEG-fMRI dataset provided by Sara Assecondi, originally acquired for other research purposes unrelated to the present thesis and described in the following.

7.2 Material and Methods

The data acquisition has been done at the facilities of CIMeC, Center for Mind/Brain Sciences,University of Trento, Italy. EEG and fMRI data have been jointly and simultaneously acquired on healthy subjets by Sara Assecondi. The decision to adopt it within the framework of the present thesis was driven by its availability and by the fact that other data were technically impossible to acquire due to technical failures of the scanner at our facility.

7.2.1 Subjects and Stimuli

Eleven subjects with no history of neurological or psychiatric disease and aged between 20 and 34 years (mean 24.8 $\pm$ 3.9 years) participated in the study, which was approved by the local Ethics Committee, with informed written consent. Data have been acquired in 4 different conditions (i.e. classes). One acquisition was in resting state condition (10

minutes) with the subject awake and not performing any specific task fixating a cross. All of the other three acquisitions were characterized by a Flashing Checkerboard of the duration of 20 seconds interleaved by 10 seconds of rest fixating a cross, this period was repeated for 12 blocks or trials. These three acquisitions differed from each other by the fact that in the first the visual checkerboard was the only stimulus while in the other two also a mental task was added during the flashing visual stimulation. This mental task consisted in a mental backward counting by one and by seven respectively. The screen had a refresh rate of 60 Hz (0,017s). The frequency of reversal for the Flashing Checkerboard was of 4 Hz. The backward counting rate was self-paced. This protocol acquisition was originally motivated to acquire data with different cognitive loadings, and thus different and modulated level of autonomic response with the aim of subsequently test advanced algorithms for ballistocardiogram artefact correction.

7.2.2 fMRI

Scans were acquired on a Bruker 4-Tesla scanner. A Circle Localiser (Coil: 8-channel) scan was performed first, followed by a MPRAGE T1-weighted anatomic scan [flip angle=7° and TI=1020 ms]. Next, we acquired functional scans over 37 slices consisting of point spread function distortion corrected (DiCo) echoplanar scan (Zaitsev et al., 2004) (EPI with voxel of 3x3x3, matrix= 64x64, axial(10°), TE/TR=(33/2200), Time of Acquisition=387s, for a total of 176 volumes. Finally the acquisition for the resting state data was of functional scans with a point spread function distortion corrected (DiCo) echoplanar scan (Zaitsev et al., 2004) (voxel of 3x3x3, matrix= 64x64, 37 slices, axial(10°), TE/TR=(33/2200), Time of Acquisition=605s, for a total of 275 volumes. Ten "dummy" scans were performed for all acquisition at the beginning to allow for longitudinal equilibrium, after which the paradigm was automatically triggered to start by the scanner.

7.2.3 EEG

The EEG acquisition has been performed with a fully magnetic compatible EEG system (Brain Products GmbH, Gilching, Germany). A 64-channel cap (equidistant 64 channels arrangement with 62 unipolar EEG channels) with sampling rate of 5000 Hz was used, the ECG electrode was placed on the left upper torso.

7.2.4 Preprocessing

Both fMRI and EEG data were preprocessed using Matlab (Mathworks, Natick, Massachussets). In particular fMRI data were preprocessed using SPM software (`http://www.fil.ion.ucl.ac.uk/spm/`). The preprocessing included slice timing correction, realignment, co-registration of anatomical image to functional image, segmentation of tissues, normalization to an MNI standard template and spatial smoothing with gaussian kernel of 6 mm. In this way all the subjects were directly comparable. The preprocessing for the EEG data included the correction for artefacts due to the magnetic field and simultaneous fMRI acquisition and BCG noise due to cardiac activity. The gradient and BCG artefacts were corrected using the EEGLAB toolbox (Delorme and Makeig, 2004) and its plug-in FMRIB (Niazy et al., 2005), the algorithm used for BCG subtraction was Average Artifact Subtraction (Allen et al., 1998) as implemented in the FMRIB plug-in. The EEG data was then down-sampled to 256 Hz.

7.2.5 Higher Order Partial Least Square

With the aim of performing a data fusion of informative content present in the two simultaneously acquired datasets, an advanced state of the art methodological techniques has been exploited: HOPLS (we refer to (Zhao et al., 2012) for an exhaustive description of the method and full mathematical tractation). HOPLS is an extension of Partial Least Square (PLS) technique (Martinez-Montes et al., 2004). PLS is able to decompose two matrices (X and Y) via projecting the data in a common unknown latent space while at the same time maximizing the pairwise covariance between the latent variables of X and Y. In this way the found hidden latent variables will make possible to predict dependent variables (i.e. data in one dataset (Y)) through the associated independent variables (i.e. data in the other dataset X). HOPLS differs mainly from PLS in way it decomposes the data (i.e. using tensorial decomposition) and in the nature of the data itself (i.e. it exploits tensors instead of mono and bidimensional vectors). HOPLS is in fact a generalized multilinear regression model which can be applied directly to tensors instead of matrices, that is it expands the properties of PLS to the domain of multidimensional (i.e. tensorial) data.

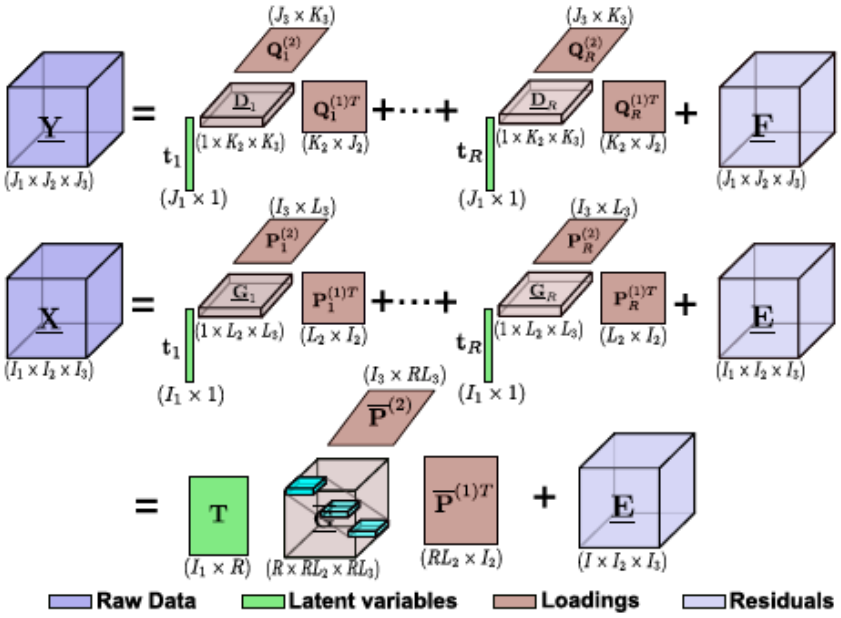

Figure 7.1: Experiment 4- Scheme of HOPLS model - In this scheme taken from (Zhao et al., 2012) the principles of HOPLS are described. Two tensorial datasets are decomposed as a sum of rank-$(1;L2;L3)$ tensors. The common latent variables are included in T. The size of the first dimension is the same for both datasets.

In practice, as it is described in Figure 7.1, we consider two tensors X and Y, one independent and one dependent, with X of order N and Y of order M. X could for example represent fMRI dataset (of dimensions trials by subjects by voxels by time points by classes) and Y could be the EEG dataset (of dimensions trials by subjects by channels by time points by frequencies by classes). Both of them have a dimension of the same size that is $I1 = J1$, in our examples the number of trials. It is then possible to apply HOPLS in order to identify a common subspace in which latent vectors from X and Y have maximum pairwise covariance. If we consider linearity in the relationship between tensors the solution is to find a common latent subspace which can approximate both X and Y simultaneously. In this case matrices P and Q in Figure 7.1 will be the factors associated to the latent variable which will describe how the latent variables reflects into the various different domains.

The code for HOPLS has been furnished by Qibin Zhao during a collaborative intership at Prof. Cichocki's laboratory (RIKEN institute, Tokyo). It is worth noting that computational needs to run experiments with data as huge as fMRI and EEG are particularly demanding.

7.2.6 Data Fusion with HOPLS and Classification

Given the description of the HOPLS method it is then possible to rearrange the acquired data to have a common dimension of the same size. This is effectively the only constraint of the method to satisfy. In our case it is possible to obtain for each subject a tensor from fMRI data (tensor X)arranging them in *trials* by *voxels* by *timepoints* by *classes*, while for EEG data (tensor Y) we obtain *trials* by *channels* by *timepoints* by *frequencies* by *classes*.

In order to improve interpretability we then used FastICA to extract ICs separately in spatial fMRI domain, temporal fMRI domain, spatial EEG domain and temporal EEG domain. Each of these ICs can then be identified, linked and associated to all the others ICs in different domains with minimal assumptions about a priori knowledge and models since the exploitation of HOPLS core tensor permit us to intrinsically identify the relationships between ICs extracted via absorption of loading matrix of each ICA decomposition into the core tensor. The result will be a set of ICs in each domain in each modality with the weights of the links representing the relationships among them. We then applied this method to a classification task which permitted

us to identify latent variables, link between EEG and fMRI, ranking of component in terms of relevance to accuracy of classification and identification of component more discriminative between tasks.

Moreover, since we are decomposing data which can be grouped in 4 different *classes*, it is possible to consider HOPLS method as a feature extraction algorithm and exploit the features, i.e. the latent variables, to classify the data according to the different stimuli. The idea is that if it is possible to correctly classify the data using latent variables common to both fMRI and EEG data, those variables will be relevant to the problem and they will work as a link between the associated information in the other dimensions of fMRI and EEG data, thus making a connection between these two different datasets. In other words it should be possible to see how much the latent variables are discriminative, i.e. if they contain information, and how these discriminative components manifest themselves in the dimensions of EEG and fMRI tensors. This means that given the same common latent variable, there will be an associated fMRI spatial map, fMRI time course as much as an associated EEG topography, EEG time course and EEG frequency spectrum. This approach permits to overcome the issue of haemodynamic modelization, dealing with the entire problem under machine learning and information theory perspectives.

7.3 Preliminary Results

In this section we report some preliminary results obtained from the analysis. Three different classifications have been performed using HOPLS based Discriminant Analysis applied to fMRI only, EEG only and EEG-fMRI data. The classification is performed with leave-one-out cross-validation on the extracted latent variables. The number of extracted latent variables has been heuristically chosen to be of 50. Table 7.1 reports the obtained results.

	fMRI	EEG	EEG-fMRI
Classification Accuracy (50 latent variables)	100%	30%	83%

Table 7.1: Experiment 4: Accuracy of classification - This table summarizes the performance results in terms of accuracy of classification using HOPLS Discriminant Analysis. The classifier is applied with cross-validation to fMRI only, EEG only and EEG-fMRI data for 4 classes and 5 subjects.

Given one latent variable, it is possible to visualize how it manifests into the fMRI domains, i.e. the associated spatial map, as well as in the corresponding EEG domains, i.e. topography, time course and frequency spectra. Figure 7.2 reports an example of the visualization of the results, that is how the component reflects in the different dimensions of different datasets the most discriminative of the 50 extracted latent variables. It is possible to see the Independent Components, linked via the most discriminative latent variable, of the fMRI spatial map, EEG topography, EEG time course and EEG spectra for one subject.

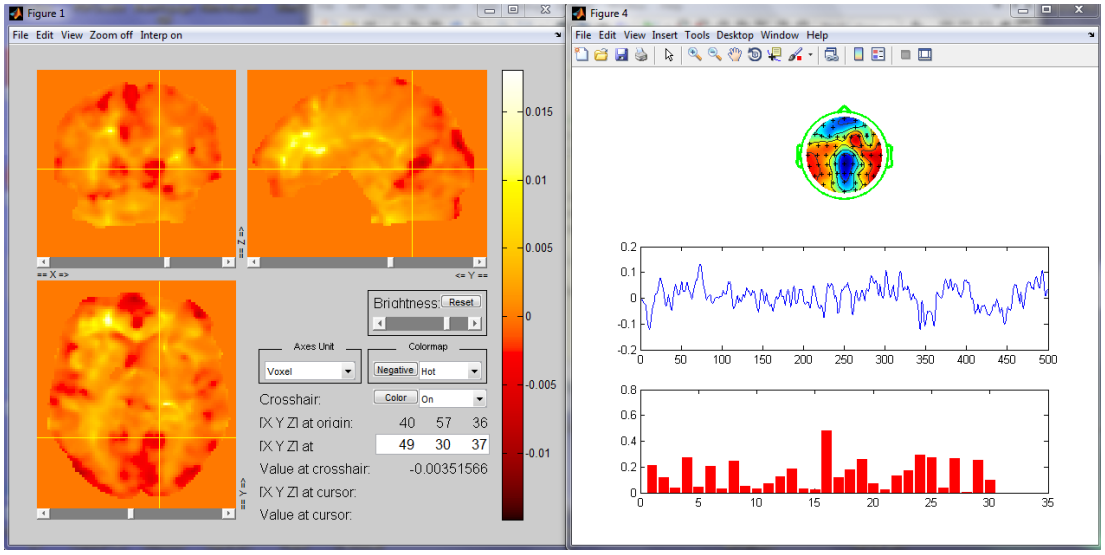

Figure 7.2: Experiment 4- Example of HOPLS-derived associated components - In this figure an example of results is reported. The components associated to one latent variable in different domains are reported. The fMRI spatial map and the corresponding (through the latent variable) EEG topography, time course [samples] and frequency spectra [Hz] from preliminary results are reported as exemplification.

7.4 Discussion

Although very preliminary, the obtained results shed the lights on different aspects of the presented method. First of all, they show the feasibility of the method and the interesting exploitation of HOPLS for data fusion, making it possible to see how the same latent variable reflects in different types of data. In particular this approach, based on information theory and exploiting the organization of the data in tensors, makes it possible to ignore the problem of the haemodynamic response, which is a big obstacle to the fusion of data coming from two different sources such as fMRI and EEG data. However, the aim of the study was also to evaluate if the spatial maps, topography, time courses and spectra were also meaningful and reliable. With this aim the classification perspective has been developed in order to have a metric to state how much the results were reliable. The rationale is that if the latent variable can be discriminative it means that they convey relevant information, thus their associated component in fMRI and EEG data dimensions were reliable. Unfortunately these preliminary results show that in the EEG dimension alone the classifier performs poorly (30%), thus not fully justi-

fying the assumption. This can be due to the lack of informative content at the level of EEG to make it possible to discriminate between conditions as close to each other as in the adopted dataset. In particular the underlying flashing checkerboard always present in each task would probably add to much variance to be solved by the simple classifier adopted in the present experiment. In fact the joint classification exploiting both types of data shows that the classification accuracy decreases with respect to that based on fMRI data alone, which performs very well (100%). This means that the result of the joint classification is strongly biased by the fMRI data, while the EEG contribution presumably negligible. Thus, although the EEG components are directly linked to fMRI data, their reliability is low in this case. It is then possible to state that for this problem, the dataset adopted is ill-posed with respect to the exploited classifier, thus making it difficult to assess if it contains enough discriminative information to justify the claim done that the linked components in EEG and fMRI are effectively meaningful and reliable.

Further work will certainly include both the selection of a more suitable dataset and the investigation of different and more advanced classification techniques, in order to fully disambiguate the possibility that the poor performance of the classification in the case of EEG data are due to the classifier and not to the informative content of the data.

7.5 Conclusions

In this chapter a novel approach to the data fusion of EEG and fMRI data is proposed, with some preliminary results obtained from simulations. Although being promising, the method has been applied to a jointly acquired EEG-fMRI dataset which was from a theoretical perspective not optimal for the intended goal. It remains to be further investigated whether the adoption of different classification techniques or different tasks in the acquisition of data can overcome the identified limitations. Moreover future work needs to be dedicated to the interpretation of the results, which could make much more sense in relation to a more suitable dataset acquired to answer a specific cognitive question.

8

Conclusions and future work

In the current chapter the conclusions are drawn about the work described in the thesis, along with a summary descriptions of main procedures, findings and results. Future work is proposed in the perspective of the state of the art research with real-time neuroscience methods.

The present thesis describes methodological work done in order to implement algorithms for real-time signal processing. The first goal in order to do so has been to implement a framework which permits the acquisition and analysis of fMRI data within our facility. This has been achieved exploiting a combination of a scanner acquisition sequence adapted to real-time and software written in the easy portable Matlab programming language. The sequence exports Point Spread Function corrected fMRI volumes to a shared folder, from which three separated in-house developed Matlab software import into a buffer the data on the fly, perform the processing of the data and visualize the results.

The second target of the thesis was to implement novel real-time methods. Novel methods in real-time fMRI are necessary to overcome current limitations and to improve the quality of the results which can be obtained. In particular a great limitation is that current real-time fMRI methods do not permit to follow the dynamic changes in the structure of brain activations. In order to do so an adaptive signal processing technique, such as ICA must be exploited. For this reason ICA has been selected as the workhorse of the present thesis. With the aim of implementing novel ICA-based method it has

been necessary to reach two goals: i) the selection of the optimal ICA algorithm between the numerous presented in literature, and ii) the way it can be exploited into a practical implementation.

The first issue has been addressed via a parametric comparison of 14 algorithms proposed in literature evaluating and quantifying i)if ICA can suit the constraints of real-time experiments, ii) which ICA algorithm is more suitable for real-time experiments, and iii) which are the optimal parameters to perform such kind of analysis. We tested the methods on publicly available fMRI data acquired on healthy subjects performing a visuo-motor task, described in the Appendix. Comparing various algorithms we show that ICA can satisfactory work in ill-posed conditions typical of real-time, with results which are similar and thus acceptable with respect to the off-line implementation. Performance was evaluated by computing the spatial and temporal correlation to a target component as well as computation time. Four algorithms were identified as best performing without prior information (constrained ICA, fastICA, jade-opac and evd), with their corresponding parameter choices. Both spatial and temporal priors are found to almost double the similarity to the target at not computation costs for the constrained ICA method and the best performing algorithms (evd, constrained ICA) show to be robust against errors in parameters, and fast in terms of computational time. It is worth noting that the parameter choices, in particular the length of the window, are driven mainly by the period of the activation investigated, thus making it optimal a size of the window comparable to the period of activation.

The identified optimal ICA algorithms can thus be exploited as core functions for the implementation of sliding-window ICA-based methods to perform real-time fMRI analysis. This is the second issue and the core of the dissertation. Several novel methods are proposed, which are able to follow the brain activation of interest by exploiting in different manner the spatial, temporal or spatio-temporal *a priori* knowledge, when available. Four different methods are proposed i) back-projection of constant spatial information derived from a functional localizer, ii) dynamic use of temporal, iii) spatial, or both iv) spatial-temporal ICA constrained data. We tested the methods on the publicly available fMRI dataset which is detailed in the Appendix. The methods were evaluated based on spatial and/or temporal correlation with the target IC component monitored, computation time and intrinsic stochastic variability of the algorithms. The method that gave the highest performance was based on the back-projection of

a constant target spatial map derived by the spatial localizer. This method has the limitation that its reference is constant and may not be optimal to follow as it cannot adapt to changes in the brain activation. The other tested methods were based on the use of adaptive spatial, temporal or spatial-temporal priors and may have useful applications in studies where there is a need of higher flexibility to monitor variable activation, such as neurofeedback studies.

The last goal of the thesis was to overcome the natural limitation of fMRI as a slow neuroimaging technique via exploiting multimodal neuroimaging and proposing a novel data fusion algorithm. Indeed, the recent possibility to acquire EEG data within the MR environment while simultaneously recording fMRI data makes it possible to think about the possibility of exploiting joint acquisition to take advantage of both high spatial and temporal resolution of the two techniques. Technical challenges are obviously present, in particular due to artefacts caused by fMRI acquisition and induced onto EEG dataset and to safety issues for the subject, and are solved by the use of advanced algorithms for the correction of gradient and ballistocardiogram artefacts and by particular protocols and care during acquisition of data. Despite this challenges, a great effort must be spent into the development of methods to actually extract and exploit the information present in these heterogeneous datasets.

The problem of data fusion is faced here from the perspective of information theory, via proposing the exploitation of a novel PLS method called Higher Order Partial Least Square. Within HOPLS framework the dataset from EEG and fMRI acquisitions are decomposed through common predictors, called latent variable. These latent variables works as links between different domains of the two dataset, thus connecting for example EEG time course of the component associated to one latent variable to the correspondent fMRI spatial map, exploiting the strength of the two different modalities. The two dataset are treated as tensors, keeping their original cardinality in all the dimensions, and decomposed with tensorial decomposition techniques. In this way different domains are linked to the same latent variable for both EEG and fMRI, making it possible to exploit all the combinations between different data type and domains. The method was tested on jointly acquired EEG-fMRI data on healthy subject performing cognitive tasks of different intensity, that is performing backward counting by zero, one and seven while seeing a flashing checkerboard, as well as at rest

(fixation cross, eyes open). We found evidence that this method is promising, making it possible to obtain results from the analysis along with visualization of them in a more complete way with plots from all the different domains. It is worth noting that a more extensive test and evaluation is needed on different datasets to make claims about stability and reliability more consistent and in order to avoid the risk that the most informative neuroimaging technique actually drive the decomposition, using the other to just explain variance simply as it would do using random noise.

In agreement with previous studies we found that ICA is a technique which can suit the constraints of real-time framework. Moreover we extended this knowledge to different ICA algorithms and exploit them to implement novel methods. The novel implemented methods showed to be very promising and future work include to test them in research applications. In particular these method can be readily applied to address several different experimental question, using them in different context such BCI, neurofeedback or quality monitoring. Thanks to the flexibility of the implementation, these algorithms can also in principle be applied independently of the nature of the data, thus making them adoptable also with different neuroimaging acquisition techniques such as Near Infrared Spectroscopy or Magnetoencephalography. The investigation of their application in these different frameworks would be very interesting and worth exploring, so that to even further increase the set of tools made available to researchers.

Similarly, more effort should be devoted to the extension of preliminary results obtained with HOPLS-based data fusion method. This method, despite the underlined limitations can be very interesting under different perspectives. First of all it can become a very informative way to investigate intrinsic connectivity across modalities, via the exploitation of latent variables and application to appropriate datasets. Moreover it can be in principle applied even to other modalities to further exploring how the same information manifests in different data domains and how different domains concur to add peculiar informative contents to the framework when other modalities cannot contribute.

Finally it is of invaluable scientific interest the possibility to exploit HOPLS as a training step of a multimodal real-time neuroimaging technique. In this perspective HOPLS could be applied off-line as a functional localiser in order to identify in the

various modalities the brain activations of interest. Those activation could be then exploited in real-time monitoring applications and methods, such as those proposed by the present thesis.

9

Appendix

In this Appendix the description of the fMRI dataset used in the simulations of *Chapters 5* and *6* is reported, with details about the cognitive experiment used, the acquisition parameters, the preprocessing adopted and the computer used to perform the analysis.

9.1 fMRI Experiment Dataset

The simulation studies is based on data acquired in a real fMRI experiment (Calhoun et al., 2003). This data set (3 male healthy subjects of mean age 20 years old) was chosen because it activates a variety of well-known networks (including Default Mode, right visual/motor and left visual/motor areas) and the ICA characterization of the task-induced activation networks has been extensively studied with ICA since it is part of the public distribution of the Group ICA of fMRI toolbox (GIFT: `http://mialab.mrn.org/software/gift/index.html`). The dataset is thus publicly available and in the release it is stated that The Johns Hopkins Institutional Review Board approved the protocol and all participants provided written informed consent. The dataset is fully described in the original publication and here we outline only the main aspects related to the cognitive tasks, data acquisition and preprocessing.

9.2 Cognitive Tasks

The GIFT package contains three subjects example data-sets that employ a visuomotor paradigm derived from other studies (Calhoun et al., 2001). The visual-motor paradigm contains two identical but spatially offset, periodic, visual stimuli, shifted by 20 seconds

from one another (Figure 9.1). The visual stimuli were projected via an LCD projector onto a rear-projection screen subtending approximately 25 degrees of visual field, visible via a mirror attached to the MRI head coil. The stimuli consisted of an 8 Hz reversing checkerboard pattern presented for 15 seconds in the right visual hemi-field, followed by 5 seconds of an asterisk fixation, followed by 15 seconds of checkerboard presented to the left visual hemi-field, followed by 20 seconds of an asterisk fixation. The 55 second set of events was repeated four times for a total of 220 seconds. The motor stimuli consisted of participants touching their right thumb to each of their four fingers sequentially, back and forth, at a self-paced rate using the hand on the same side on which the visual stimulus is presented. fMRI data from this paradigm, when analyzed with standard ICA (Calhoun et al., 2003), separate activation network results into several resting state components and two different task-related components (one in left visual and motor cortex, one in right visual and motor cortex).

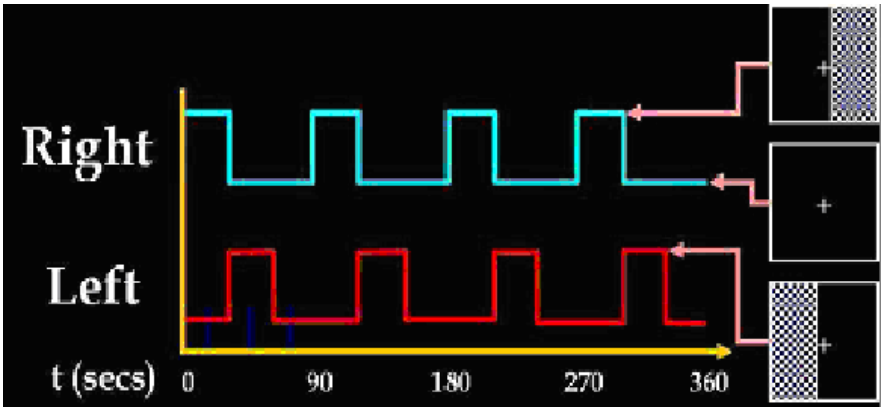

Figure 9.1: Appendix- Stimulus Set-up for acquisition of data used in Experiments 2 and 3 - The figure shows a summary of the stimulus set-up presented to the subject during experimental data acquisition.

For the purpose of our rt-fMRI simulations each subject's functional run was used in three different ways, as discussed in more details below: i) the whole time series was used to generate task-related network templates used for the estimation of accuracy of the networks estimated dynamically along the time course; ii) the first 60 TRs of the time series were considered as functional localizer FL for the estimation of target ICs to later monitor dynamically; and iii), after the FL period the rest of the time course

was used to dynamically monitor the FL-derived target ICs using a sliding-window approach.

9.3 Imaging Parameters

Scans were acquired on a Philips NT 1.5-Tesla scanner. A sagittal localizer scan was performed first, followed by a T1-weighted anatomic scan [repeat time (TR) = 500 ms, echo time (TE) = 30ms, field of view = 24cm, matrix = 256 x 256, slice thickness = 5 mm, gap = 0.5 mm] consisting of 18 slices through the entire brain including most of the cerebellum. Next, we acquired functional scans over the same 18 slices consisting of a single-shot, echoplanar scan (TR = 1 s, TE = 39 ms, field of view = 24 cm, matrix = 64 x 64, slice thickness = 5 mm, gap = 0.5 mm, flip angle = 90 degrees) obtained consistently over a 3-min, 40-s period for a total of 220 scans. Ten "dummy" scans were performed at the beginning to allow for longitudinal equilibrium, after which the paradigm was automatically triggered to start by the scanner.

9.4 Preprocessing

The data used in this study were previously preprocessed. The fMRI data were first corrected for timing differences between the slices using windowed Fourier interpolation to minimize the dependence upon the reference slice chosen. Next, the data were imported into the statistical parametric mapping software package, SPM99. Data were motion corrected, spatially smoothed with a 6 x 6 x 10 mm Gaussian kernel, and spatially normalized into the standard space of Talairach. The data (originally collected at 3.4 x 3.4 x 5 mm) were slightly subsampled to 3 x 3 x 5 mm, resulting in 53 x 63 x 28 voxels.

9.5 Software and Computer for ICA Simulations

The entire simulation work is based on an in-house Matlab implementation (`http://www.mathworks.com/products/matlab`) that exploits the code available with the GIFT toolbox (GIFT,`http://mialab.mrn.org/software/gift`). Given the ICA algorithms code present in the toolbox, all the data analysis steps have been implemented

in an automatic fashion to permit a testing routine to be run on ICA algorithms varying their parameters (i.e. varying the window length, the model order, the *a priori* knowledge, and the subjects). The PC adopted to run the simulations was an Intel(R) Core(TM) i5 CPU M460 @2.53GHz equipped with 6 GB of RAM and running a Windows 7 64-bit OS.

References

Allen, P. J., Polizzi, G., Krakow, K., Fish, D. R., Lemieux, L., Oct. 1998. Identification of eeg events in the mr scanner: The problem of pulse artifact and a method for its subtraction. NeuroImage 8 (3), 229–239.
URL http://www.sciencedirect.com/science/article/pii/S1053811998903615 73

Angelone, L. M., Potthast, A., Segonne, F., Iwaki, S., Belliveau, J. W., Bonmassar, G., 2004. Metallic electrodes and leads in simultaneous eeg-mri: Specific absorption rate (sar) simulation studies. Bioelectromagnetics 25 (4), 285–295.
URL http://dx.doi.org/10.1002/bem.10198 16

Assecondi, S., Hallez, H., Staelens, S., Bianchi, A. M., Huiskamp, G. M., Lemahieu, I., 2009. Removal of the ballistocardiographic artifact from eeg-fmri data: a canonical correlation approach. Physics in Medicine and Biology 54 (6), 1673.
URL http://stacks.iop.org/0031-9155/54/i=6/a=018 69

Babiloni, F., Cincotti, F., Babiloni, C., Carducci, F., Mattia, D., Astolfi, L., Basilisco, A., Rossini, P., Ding, L., Ni, Y., Cheng, J., Christine, K., Sweeney, J., He, B., Jan. 2005. Estimation of the cortical functional connectivity with the multimodal integration of high-resolution eeg and fmri data by directed transfer function. NeuroImage 24 (1), 118–131.
URL http://www.sciencedirect.com/science/article/pii/S1053811904005646 69

Bashashati, A., Fatourechi, M., Ward, R. K., Birch, G. E., 2007. A survey of signal processing algorithms in brain-computer interfaces based on electrical brain signals. Journal of Neural Engineering 4 (2), R32.
URL http://stacks.iop.org/1741-2552/4/i=2/a=R03 1, 21

Beckmann, C. F., Smith, S. M., Feb. 2004. Probabilistic independent component analysis for functional magnetic resonance imaging. IEEE Transactions on Medical Imaging 23 (2), 137–152.
URL http://dx.doi.org/10.1109/TMI.2003.822821 23

Bell, A. J., Sejnowski, T. J., Nov 1995. An information-maximization approach to blind separation and blind deconvolution. Neural Comput 7 (6), 1129–1159. 23, 25

Calhoun, V., Adali, T., march-april 2006. Unmixing fmri with independent component analysis. Engineering in Medicine and Biology Magazine, IEEE 25 (2), 79 – 90. 2, 23

Calhoun, V., Silva, R., Liu, J., 2007. Identification of multimodal mri and eeg biomarkers using joint-ica and divergence criteria. In: Machine Learning for Signal Processing, 2007 IEEE Workshop on. pp. 151–156. 70

Calhoun, V. D., Adali, T., Pearlson, G. D., Pekar, J. J., May 2001. Spatial and temporal independent component analysis of functional mri data containing a pair of task-related waveforms. Hum Brain Mapp 13 (1), 43–53. 23, 36, 59, 87

Calhoun, V. D., Adali, T., Pekar, J. J., Pearlson, G. D., Nov 2003. Latency (in)sensitive ica. group independent component analysis of fmri data in the temporal frequency domain. Neuroimage 20 (3), 1661–1669. 37, 41, 87, 88

Calhoun, V. D., Eichele, T., Pearlson, G., 2009. Functional brain networks in schizophrenia: a review. Frontiers in Human Neuroscience 3 (0).
URL http://www.frontiersin.org/Journal/Abstract.aspx?s=537&name=human_neuroscience&ART_DOI=10.3389/neuro.09.017.2009 23

Cichocki, A., Amari, S., 2002. Adaptive blind signal and image processing: learning algorithms and applications. No. v. 1. J. Wiley.
URL http://books.google.it/books?id=uadTAAAAMAAJ 33

Cichocki, A., Washizawa, Y., Rutkowski, T., Bakardjian, H., Phan, A.-H., Choi, S., Lee, H., Zhao, Q., Zhang, L., Li, Y., 2008. Noninvasive bcis: Multiway signal-processing array decompositions. Computer 41 (10), 34–42. 20

Correa, N., Adali, T., Calhoun, V. D., Jun 2007. Performance of blind source separation algorithms for fmri analysis using a group ica method. Magn Reson Imaging 25 (5), 684–694.
URL http://dx.doi.org/10.1016/j.mri.2006.10.017 31

Correa, N., Adali, T., Li, Y.-O., Calhoun, V. D., 2005. Comparison of blind source separation algorithms for fmri using a new matlab toolbox: Gift. In: Proc. IEEE Int. Conf. Acoustics, Speech, and Signal Processing (ICASSP '05). Vol. 5. 31, 33

Cox, R. W., Jesmanowicz, A., Hyde, J. S., Feb 1995. Real-time functional magnetic resonance imaging. Magn Reson Med 33 (2), 230–236. 2, 22

Daunizeau, J., Laufs, H., Friston, K. J., 2010. Eeg-fmri information fusion: Biophysics and data analysis. In: Mulert, C., Lemieux, L. (Eds.), EEG - fMRI. Springer Berlin Heidelberg, pp. 511–526, 10.1007/978-3-540-87919-0_25.
URL http://dx.doi.org/10.1007/978-3-540-87919-0_25 70

De Martino, F., Valente, G., de Borst, A. W., Esposito, F., Roebroeck, A., Goebel, R., Formisano, E., Oct. 2010. Multimodal imaging: an evaluation of univariate and multivariate methods for simultaneous eeg-fmri. Magnetic Resonance Imaging 28 (8), 1104–1112.
URL http://www.sciencedirect.com/science/article/pii/S0730725X0900318X 69

Debener, S., Ullsperger, M., Siegel, M., Engel, A. K., Dec. 2006. Single-trial eeg-fmri reveals the dynamics of cognitive function. Trends in Cognitive Sciences 10 (12), 558–563.
URL http://www.sciencedirect.com/science/article/pii/S1364661306002725 15, 69

Debener, S., Ullsperger, M., Siegel, M., Fiehler, K., von Cramon, D. Y., Engel, A. K., 2005. Trial-by-trial coupling of concurrent electroencephalogram and functional magnetic resonance imaging identifies the dynamics of performance monitoring. The Journal of Neuroscience 25 (50), 11730–11737.
URL http://www.jneurosci.org/content/25/50/11730.abstract 15

deCharms, R. C., Sep 2008. Applications of real-time fmri. Nat Rev Neurosci 9 (9), 720–729.
URL http://dx.doi.org/10.1038/nrn2414 21, 23

deCharms, R. C., Maeda, F., Glover, G. H., Ludlow, D., Pauly, J. M., Soneji, D., Gabrieli, J. D. E., Mackey, S. C., Dec 2005. Control over brain activation and pain learned by using real-time functional mri. Proc Natl Acad Sci U S A 102 (51), 18626–18631.
URL http://dx.doi.org/10.1073/pnas.0505210102 21

Delorme, A., Makeig, S., Mar. 2004. Eeglab: an open source toolbox for analysis of single-trial eeg dynamics including independent component analysis. Journal of Neuroscience Methods 134 (1), 9–21.
URL http://www.sciencedirect.com/science/article/pii/S0165027003003479 73

DeMartino, F., Gentile, F., Esposito, F., Balsi, M., Salle, F. D., Goebel, R., Formisano, E., 2007. Classification of fmri independent components using ic-fingerprints and support vector machine classifiers. NeuroImage 34 (1), 177 – 194.
URL http://www.sciencedirect.com/science/article/pii/S1053811906009244 24, 36

Deneux, T., Faugeras, O., Dec. 2009. Eeg-fmri fusion of paradigm-free activity using kalman filtering. Neural Computation 22 (4), 906–948.
URL http://dx.doi.org/10.1162/neco.2009.05-08-793 70

Eichele, T., Calhoun, V. D., Debener, S., Jul. 2009. Mining eeg-fmri using independent component analysis. International Journal of Psychophysiology 73 (1), 53–61.
URL http://www.sciencedirect.com/science/article/pii/S0167876009000270 70

Esposito, F., Formisano, E., Seifritz, E., Goebel, R., Morrone, R., Tedeschi, G., Salle, F. D., Jul 2002. Spatial independent component analysis of functional mri time-series: to what extent do results depend on the algorithm used? Hum Brain Mapp 16 (3), 146–157.
URL http://dx.doi.org/10.1002/hbm.10034 31

Esposito, F., Seifritz, E., Formisano, E., Morrone, R., Scarabino, T., Tedeschi, G., Cirillo, S., Goebel, R., Salle, F. D., Dec 2003. Real-time independent component analysis of fmri time-series. Neuroimage 20 (4), 2209–2224. 24, 33, 36, 46, 53, 57, 64

Gembris, D., Taylor, J. G., Schor, S., Frings, W., Suter, D., Posse, S., Feb 2000. Functional magnetic resonance imaging in real time (fire): sliding-window correlation analysis and reference-vector optimization. Magn Reson Med 43 (2), 259–268. 22

Goebel, R., 2012. Brainvoyager past, present, future. NeuroImage (0), –.

URL http://www.sciencedirect.com/science/article/pii/S1053811912001000 24, 27, 29

Himberg, J., Hyvrinen, A., Esposito, F., 2004. Validating the independent components of neuroimaging time series via clustering and visualization. NeuroImage 22 (3), 1214 – 1222.
URL http://www.sciencedirect.com/science/article/pii/S1053811904001661 52

Hinds, O., Ghosh, S., Thompson, T. W., Yoo, J. J., Whitfield-Gabrieli, S., Triantafyllou, C., Gabrieli, J. D. E., Jan 2011. Computing moment-to-moment bold activation for real-time neurofeedback. Neuroimage 54 (1), 361–368.
URL http://dx.doi.org/10.1016/j.neuroimage.2010.07.060 22

Hyvrinen, A., Oja, E., 2000. Independent component analysis: algorithms and applications. Neural Netw 13 (4-5), 411–430. 23, 25

LaConte, S. M., May 2011. Decoding fmri brain states in real-time. Neuroimage 56 (2), 440–454.
URL http://dx.doi.org/10.1016/j.neuroimage.2010.06.052 21

LaConte, S. M., Peltier, S. J., Hu, X. P., Oct 2007. Real-time fmri using brain-state classification. Hum Brain Mapp 28 (10), 1033–1044.
URL http://dx.doi.org/10.1002/hbm.20326 2, 19, 22, 27

Laufs, H., Daunizeau, J., Carmichael, D., Kleinschmidt, A., Apr. 2008. Recent advances in recording electrophysiological data simultaneously with magnetic resonance imaging. NeuroImage 40 (2), 515–528.
URL http://www.sciencedirect.com/science/article/pii/S1053811907010737 16

Lemieux, L., Salek-Haddadi, A., Lund, T. E., Laufs, H., Carmichael, D., Jul. 2007. Modelling large motion events in fmri studies of patients with epilepsy. Magnetic Resonance Imaging 25 (6), 894–901.
URL http://www.sciencedirect.com/science/article/pii/S0730725X07002214 17, 70

Lin, Q.-H., Liu, J., Zheng, Y.-R., Liang, H., Calhoun, V. D., Jul 2010. Semiblind spatial ica of fmri using spatial constraints. Hum Brain Mapp 31 (7), 1076–1088.
URL http://dx.doi.org/10.1002/hbm.20919 31, 32, 36, 58

Magland, J. F., Tjoa, C. W., Childress, A. R., Apr 2011. Spatio-temporal activity in real time (star): optimization of regional fmri feedback. Neuroimage 55 (3), 1044–1053.
URL http://dx.doi.org/10.1016/j.neuroimage.2010.12.085 22

Mantini, D., Perrucci, M. G., Del Gratta, C., Romani, G. L., Corbetta, M., 2007. Electrophysiological signatures of resting state networks in the human brain. Proceedings of the National Academy of Sciences 104 (32), 13170–13175.
URL http://www.pnas.org/content/104/32/13170.abstract 69

Martinez-Montes, E., Valdes-Sosa, P. A., Miwakeichi, F., Goldman, R. I., Cohen, M. S., Jul. 2004. Concurrent eeg/fmri analysis by multiway partial least squares.

NeuroImage 22 (3), 1023–1034.
URL http://www.sciencedirect.com/science/article/pii/S1053811904001946 69, 70, 73

McKeown, M. J., Makeig, S., Brown, G. G., Jung, T. P., Kindermann, S. S., Bell, A. J., Sejnowski, T. J., 1998. Analysis of fmri data by blind separation into independent spatial components. Hum Brain Mapp 6 (3), 160–188. 22, 23

Menon, V., Crottaz-Herbette, S., 2005. Combined eeg and fmri studies of human brain function. International Review of Neurobiology 66, 291–321, cited By (since 1996) 25.
URL http://www.scopus.com/inward/record.url?eid=2-s2.0-33644770342&partnerID=40&md5=9b507fa135879a45fc6a5fbf7ff3796b 9, 13

Mouro-Miranda, J., Bokde, A. L. W., Born, C., Hampel, H., Stetter, M., Dec 2005. Classifying brain states and determining the discriminating activation patterns: Support vector machine on functional mri data. Neuroimage 28 (4), 980–995.
URL http://dx.doi.org/10.1016/j.neuroimage.2005.06.070 22

Mulert, C., Lemieux, L., 2009. EEG - fMRI: Physiological Basis, Technique, and Applications. Springer.
URL http://books.google.it/books?id=1UOiD94HdXkC 9, 13, 16

Niazy, R., Beckmann, C., Iannetti, G., Brady, J., Smith, S., Nov. 2005. Removal of fmri environment artifacts from eeg data using optimal basis sets. NeuroImage 28 (3), 720–737.
URL http://www.sciencedirect.com/science/article/pii/S1053811905004726 73

Norman, K. A., Polyn, S. M., Detre, G. J., Haxby, J. V., Sep 2006. Beyond mind-reading: multi-voxel pattern analysis of fmri data. Trends Cogn Sci 10 (9), 424–430.
URL http://dx.doi.org/10.1016/j.tics.2006.07.005 22

Phillips, C., Rugg, M. D., Friston, K. J., Jul. 2002. Anatomically informed basis functions for eeg source localization: Combining functional and anatomical constraints. NeuroImage 16 (3, Part A), 678–695.
URL http://www.sciencedirect.com/science/article/pii/S1053811902911432 17, 70

Posse, S., Fitzgerald, D., Gao, K., Habel, U., Rosenberg, D., Moore, G. J., Schneider, F., Mar 2003. Real-time fmri of temporolimbic regions detects amygdala activation during single-trial self-induced sadness. Neuroimage 18 (3), 760–768. 21

Purdon, P. L., Millan, H., Fuller, P. L., Bonmassar, G., Nov. 2008. An open-source hardware and software system for acquisition and real-time processing of electrophysiology during high field mri. Journal of Neuroscience Methods 175 (2), 165–186.
URL http://www.sciencedirect.com/science/article/pii/S016502700800397X 69

Robinson, S., Basso, G., Soldati, N., Sailer, U., Jovicich, J., Bruzzone, L., Kryspin-Exner, I., Bauer, H., Moser, E., 2009.

A resting state network in the motor control circuit of the basal ganglia. BMC Neuroscience 10 (1), 137.
URL http://www.biomedcentral.com/1471-2202/10/137 37

Shibata, K., Watanabe, T., Sasaki, Y., Kawato, M., 2011. Perceptual learning incepted by decoded fmri neurofeedback without stimulus presentation. Science 334 (6061), 1413–1415.
URL http://www.sciencemag.org/content/334/6061/1413.abstract 21

Sitaram, R., Lee, S., Ruiz, S., Rana, M., Veit, R., Birbaumer, N., May 2011. Real-time support vector classification and feedback of multiple emotional brain states. Neuroimage 56 (2), 753–765.
URL http://dx.doi.org/10.1016/j.neuroimage.2010.08.007 22

Soldati, N., Calhoun, V. D., Bruzzone, L., Jovicich, J., June 2012. Real-time fmri using ica: optimization study for defining a target ic from a functional localizer. 18th Annual Meeting of the Organization for Human Brain Mapping , Beijing, China. 39, 51, 54, 55

Soldati, N., Robinson, S., Persello, C., Jovicich, J., Bruzzone, L., 1 2009. Automatic classification of brain resting states using fmri temporal signals. Electronics Letters 45 (1), 19 –21. 37

Sorger, B., Reithler, J., Dahmen, B., Goebel, R., Jul. 2012. A real-time fmri-based spelling device immediately enabling robust motor-independent communication.
URL http://linkinghub.elsevier.com/retrieve/pii/S0960982212005751 1

Steriade, M., McCarley, R., 2005. Brain Control of Wakefulness and Sleep. Springer.
URL http://books.google.it/books?id=bph8MBn5KhUC 12

Sui, J., Adali, T., Li, Y.-O., Yang, H., Calhoun, V. D., 2010. A review of multivariate methods in brain imaging data fusion, 76260D–76260D–11.
URL http://dx.doi.org/10.1117/12.843922 17, 70

Thompson, T., Hinds, O., Ghosh, S., Lala, N., Triantafyllou, C., Whitfield-Gabrieli, S., Gabrieli, J., 2009. Training selective auditory attention with real-time fmri feedback. NeuroImage 47 (Supplement 1), S65 – S65, organization for Human Brain Mapping 2009 Annual Meeting.
URL http://www.sciencedirect.com/science/article/pii/S1053811909703398 21

Ullsperger, M., Debener, S., 2010. Simultaneous EEG and fMRI:Recording, Analysis, and Application: Recording, Analysis, and Application. Oxford University Press, USA.
URL http://books.google.it/books?id=HtkAfChTLToC 9, 13

Weiskopf, N., 2011. Real-time fmri and its application to neurofeedback. NeuroImage (0), –.
URL http://www.sciencedirect.com/science/article/pii/S1053811911011700 22, 23

Weiskopf, N., Klose, U., Birbaumer, N., Mathiak, K., 2005. Single-shot compensation of image distortions and bold contrast optimization using multi-echo epi for real-time fmri. NeuroImage 24 (4), 1068 –

1079.
URL http://www.sciencedirect.com/science/article/pii/S1053811904006147 28

Weiskopf, N., Mathiak, K., Bock, S., Scharnowski, F., Veit, R., Grodd, W., Goebel, R., Birbaumer, N., june 2004a. Principles of a brain-computer interface (bci) based on real-time functional magnetic resonance imaging (fmri). Biomedical Engineering, IEEE Transactions on 51 (6), 966 –970. 28

Weiskopf, N., Scharnowski, F., Veit, R., Goebel, R., Birbaumer, N., Mathiak, K., 2004b. Self-regulation of local brain activity using real-time functional magnetic resonance imaging (fmri). J Physiol Paris 98 (4-6), 357–373.
URL http://dx.doi.org/10.1016/j.jphysparis.2005.09.019 21

Weiskopf, N., Sitaram, R., Josephs, O., Veit, R., Scharnowski, F., Goebel, R., Birbaumer, N., Deichmann, R., Mathiak, K., Jul 2007. Real-time functional magnetic resonance imaging: methods and applications. Magn Reson Imaging 25 (6), 989–1003.
URL http://dx.doi.org/10.1016/j.mri.2007.02.007 21, 22, 27

Zaitsev, M., Hennig, J., Speck, O., 2004. Point spread function mapping with parallel imaging techniques and high acceleration factors: Fast, robust, and flexible method for echo-planar imaging distortion correction. Magnetic Resonance in Medicine 52 (5), 1156–1166.
URL http://dx.doi.org/10.1002/mrm.20261 29, 72

Zhao, Q., Caiafa, C. F., Mandic, D. P., Chao, Z. C., Nagasaka, Y., Fujii, N., Zhang, L., Cichocki, A., 2012. Higher-order partial least squares (hopls): A generalized multi-linear regression method. CoRR abs/1207.1230.
URL http://arxiv.org/abs/1207.1230 70, 73, 74

Zotev, V., Phillips, R., Yuan, H., Drevets, W., Bodurka, J., 2012. Simultaneous real-time fmri and eeg neurofeedback for self-regulation of human brain activity. In: 20th Annual Meeting of the International Society for Magnetic Resonance in Medicine. 27

Declaration

I herewith declare that I have produced this paper without the prohibited assistance of third parties and without making use of aids other than those specified; notions taken over directly or indirectly from other sources have been identified as such. This paper has not previously been presented in identical or similar form to any other Italian or foreign examination board.

The thesis work was conducted under the supervision of Jorge Jovicich and Lorenzo Bruzzone at the University of Trento.

Trento, December 2012